# A stable time advancing scheme for solving fluid-structure interaction problem at small structural displacements

Soyibou Sy, Cornel Marius Murea *

*Laboratoire de Mathématiques, Informatique et Applications,*

*Université de Haute-Alsace,*

*4-6, rue des Frères Lumière, 68093 MULHOUSE Cedex, France*

**Abstract**

A semi-implicit time advancing scheme for transient fluid-structure interaction problem is presented. At every time step, a least squares problem is solved by partitioned procedures, such that the continuity of the velocity as well as the continuity of the stress hold at the interface. During the iterative method for solving the optimization problem, the fluid mesh does not move, which reduces the computational effort. The stability of the algorithm is derived. The numerical results presented in this paper show that the computed solution is similar to the one obtained by the implicit algorithm, but the computational time is reduced.

*Key words:* Fluid-structure interaction, Semi-implicit time advancing scheme, Finite element

## 1 Introduction

In fluid-structure interaction problems, on the one hand, the stresses from the fluid move the structure and on the other hand, the fluid domain depends on the displacement of the structure. At the fluid-structure interface, the continuity of the stress and of the velocity are imposed. The flow inside a compliant vessel or the displacement of high buildings under the action of the wind are examples of fluid-structure interaction. We are interested in the haemodynamics applications such that the blood flow in large arteries.

Different time advancing algorithms have been developed for unsteady fluid-structure interaction: explicit, implicit and, recently, semi-implicit. In the explicit algorithms, the two coupling conditions are not verified simultaneously. For example, at a time step the continuity of the velocity holds, but the continuity of the stress across the interface is violated or inversely. Explicit algorithms have been successfully employed in aero-elasticity [8]. But, these algorithms are unstable when the structure is light and its density is comparable to that of the fluid [16], [4], [12]. Such situations appear in the bio-mechanics applications, for example.

At every time step of the implicit algorithms, the fluid domain as well as the displacement of the structure, velocity and the pressure of the fluid have to be determined by iterative methods. This can be done using fixed point strategies [21], [11], Newton or quasi-Newton methods [25], [14], [1], [9], [27],

* Corresponding author. Phone: +33 3 89 33 60 34, Fax: +33 3 89 33 66 53
*Email addresses:* soyibou.sy@uha.fr (Soyibou Sy), cornel.murea@uha.fr (Cornel Marius Murea).
*URL:* http://www.edp.lmia.uha.fr/murea/ (Cornel Marius Murea).

[6], [5]. Optimal control approaches have been employed in [19], [17] where, at each time step, an optimization problem must be solved. Contrary to Newton or fixed point iterations, the optimization approach is less sensitive to the starting point, which permits to use moderate time step. Numerical results presented in [19] suggest to use Modified Newton Method for small time step, while the optimization approach is preferable for moderate time step.

In the case of implicit algorithms, we emphasize that at a time instant, the fluid domain is changed in the interior of the loop where the structure displacement, the velocity and the pressure of the fluid are computed iteratively. The idea of semi-implicit algorithms is to compute explicitly the fluid domain out of the loop, then a frozen fluid mesh is used during the iterative algorithm until both coupling conditions at the interface hold. This strategy reduces the computational time.

A semi-implicit algorithm for a mono-dimensional simplified fluid-structure interaction problem is introduced in [13] and the stability in time is proved. In [21, Sec. 4.10, p. 138] a semi-implicit algorithm based on the Leap-Frog discretisation for the structure and on the implicit Euler discretisation for the fluid is presented. In order to linearize the convection term of Navier-Stokes equation, a supplementary fluid problem has to be solved. The stability is proved under a condition on the time step governed only by the structure. The author remarks at p. 140 that this condition might to be too restrictive in haemodynamics applications. The stability analysis of semi-implicit algorithms of first order in time for fluid-structure interaction problems can be found in [2] and [26]. In [10], a semi-implicit algorithm based on the Chorin-Temam projection scheme for incompressible flows is proposed. The stability has been proved when the fluid domain is fixed. The numerical results show

that the computational time is reduced when the semi-implicit strategy is employed in place of the implicit one. Other semi-implicit algorithms are presented in [22], where the structure equation is embedded into the fluid equations and in [20], where the fluid-structure coupled problem is solved by the Augmented Lagrangian Method.

The aim of this paper is to introduce a different semi-implicit algorithm for transient fluid-structure interaction problems. The main differences between our method and the ones proposed in [21], [2], [26] are: we use a centered scheme of order two in time for the structure and more general boundary conditions for the fluid. The unconditional stability of the algorithm is derived. Moreover, the numerical results presented in this paper show that the computed solution is similar to the one obtained by the implicit algorithm, but the computational time is reduced.

## 2 The mathematical model

We are interested in fluid-structure interaction problem in two dimensions. Let us denote by $\Omega^S$ the undeformed structure domain and we suppose that its boundary $\partial\Omega^S$ admits decomposition $\partial\Omega^S = \Gamma_D \cup \Gamma_N \cup \Gamma_0$, with $\Gamma_D = [AB] \cup [CD]$ and $\Gamma_N = [AD]$ (see Figure 1 on the left). We denote by $\Omega_0^F$ the initial fluid domain bounded by: $\Sigma_1$ the inflow section, $\Sigma_2$ the bottom boundary, $\Sigma_3$ the outflow section and $\Gamma_0$ the top boundary. The boundary $\Gamma_0$ is common to both domains and it represents the fluid-structure interface. Under the action of the fluid stress, the structure will be deformed. At the time instant $t$, the fluid occupies the domain $\Omega_t^F$ bounded by the moving interface $\Gamma_t$ and by the rigid boundary $\Sigma = \Sigma_1 \cup \Sigma_2 \cup \Sigma_3$ (see Figure 1 at the right).

We assume that the fluid is viscous, Newtonian and incompressible and it is governed by the Navier-Stokes equations. We also assume that the structure is governed by the linear elasticity equations. The coupling between the fluid and the structure is realized through two boundary conditions at the interface, namely, the continuity of the velocity and the equality of the stress. At each time $t \in [0, T]$, we are interested to know: the fluid velocity $\mathbf{v}(t) = (v_1(t), v_2(t))^T : \Omega_t^F \longrightarrow \mathbb{R}^2$, the fluid pressure $p(t) : \Omega_t^F \longrightarrow \mathbb{R}$ and the structure displacement $\mathbf{u}(t) = (u_1(t), u_2(t))^T : \Omega^S \longrightarrow \mathbb{R}^2$.

We are going to use the ALE (Arbitrary Lagrangian Eulerian) coordinates for the fluid equations, see for example [23]. Let $\widehat{\Omega}^F$ be the reference fixed domain and let $\mathcal{A}_t, t \in [0, T]$ be a family of transformations such that:

$$\mathcal{A}_t(\widehat{\mathbf{x}}) = \mathbf{x}, \ \forall \ \widehat{\mathbf{x}} \in \widehat{\Omega}^F, \ \mathcal{A}_t(\widehat{\Omega}^F) = \Omega_t^F,$$

where $\widehat{\mathbf{x}} = (\widehat{x}_1, \widehat{x}_2)^T \in \widehat{\Omega}^F$ are the ALE coordinates and $\mathbf{x} = (x_1, x_2)^T \in \Omega_t^F$ are the Eulerian coordinates. We denote the domain velocity by:

$$\boldsymbol{\vartheta}(\mathbf{x}, t) = \frac{\partial \mathcal{A}_t}{\partial t}(\widehat{\mathbf{x}}) = \frac{\partial \mathcal{A}_t}{\partial t}\left(\mathcal{A}_t^{-1}(\mathbf{x})\right)$$

and the ALE time derivative of the fluid velocity by:

$$\left.\frac{\partial \mathbf{v}}{\partial t}\right|_{\widehat{\mathbf{x}}}(\mathbf{x}, t) = \frac{\partial \widehat{\mathbf{v}}}{\partial t}(\widehat{\mathbf{x}}, t).$$

We assume that the fluid-structure interaction is governed by the following equations:

*Navier-Stokes*

$$\rho^F \left( \left. \frac{\partial \mathbf{v}}{\partial t} \right|_{\widehat{\mathbf{x}}} + ((\mathbf{v} - \boldsymbol{\vartheta}) \cdot \nabla) \mathbf{v} \right) - 2\mu^F \nabla \cdot \epsilon(\mathbf{v}) + \nabla p = \mathbf{f}^F, \ \Omega_t^F \times (0,T] \quad (1)$$

$$\nabla \cdot \mathbf{v} = 0, \ \Omega_t^F \times [0,T] \quad (2)$$

$$\sigma^F \mathbf{n}^F = \mathbf{h}_{in}, \ \Sigma_1 \times (0,T] \quad (3)$$

$$\sigma^F \mathbf{n}^F = \mathbf{h}_{out}, \ \Sigma_3 \times (0,T] \quad (4)$$

$$\mathbf{v} = 0, \ \Sigma_2 \times (0,T] \quad (5)$$

$$\mathbf{v}(X,0) = \mathbf{v}^0(X), \ \Omega_0^F \quad (6)$$

*linear elasticity*

$$\rho^S \frac{\partial^2 u}{\partial t^2} - \nabla \cdot \sigma^S = \mathbf{f}^S, \quad \text{in } \Omega^S \times (0,T] \quad (7)$$

$$\mathbf{u} = 0, \quad \text{on } \Gamma_D \times (0,T] \quad (8)$$

$$\sigma^S \mathbf{n}^S = 0, \quad \text{on } \Gamma_N \times (0,T] \quad (9)$$

$$\mathbf{u}(X,0) = \mathbf{u}^0(X), \quad \text{in } \Omega^S \quad (10)$$

$$\frac{\partial \mathbf{u}}{\partial t}(X,0) = \dot{\mathbf{u}}^0(X), \quad \text{in } \Omega^S \quad (11)$$

*interface conditions*

$$\mathbf{v}(X + \mathbf{u}(X,t), t) = \frac{\partial \mathbf{u}}{\partial t}(X,t), \quad \text{on } \Gamma_0 \times (0,T] \quad (12)$$

$$(\sigma^F \mathbf{n}^F)_{(X+\mathbf{u}(X,t),t)} \omega = -(\sigma^S \mathbf{n}^S)_{(X,t)}, \quad \text{on } \Gamma_0 \times (0,T]. \quad (13)$$

We have used the following notations:

$$\epsilon(\mathbf{v}) = \frac{1}{2}\Big(\nabla \mathbf{v} + (\nabla \mathbf{v})^T\Big), \ \sigma^F = -p\mathbb{I}_2 + 2\mu^F \epsilon(\mathbf{v}), \ \sigma^S = \lambda^S (\nabla \cdot \mathbf{u})\mathbb{I}_2 + 2\mu^S \epsilon(\mathbf{u}),$$

$\rho^F > 0$ is the mass density of the fluid ($\rho^S > 0$ the mass density of the structure), $\mu^F$ is the viscosity of the fluid ($\mu^S$ and $\lambda^S$ are the Lamé coefficients), $\mathbf{f}^F = (f_1^F, f_2^F)$ are the applied volume forces of the fluid, in general the gravity forces, ($\mathbf{f}^S = (f_1^S, f_2^S)$ the applied volume forces on the structure), $\mathbf{h}_{in}$ ($\mathbf{h}_{out}$) is the prescribed boundary stress on $\Sigma_1$ (on $\Sigma_3$), $\omega = \|\mathrm{cof}(\nabla \mathbb{T}_u)\mathbf{n}^S\|_{\mathbb{R}^2}$, where $\mathbb{T}_u$ is the mapping from $\Gamma_0$ in $\Gamma_t$ defined by: $\mathbb{T}_u(X) = X + \mathbf{u}(X,t)$, $\mathrm{cof}(\nabla \mathbb{T}_u)$

is the co-factor matrix of $\nabla \mathbb{T}_u$ and $\mathbf{n}^S = (n_1^S, n_2^S)$ is the unit outward normal to $\Gamma_0$.

**Remark 1** *In the system (1)–(13), the fluid and the structure are treated differently: on the one hand, the structure is governed by a linear elastic constitutive law adapted for small deformations and, on the other hand, the fluid equations are written in a moving domain. We are motivated by haemodynamics applications and for instance we study numerically the blood flow in a segment of artery of 6 cm length, 0.1 cm thickness and 1 cm diameter. In the real life, the deformation of the artery is about 0.1 cm and a linear mathematical model for the structure could be sufficient. Contrary to the elastic solids, the fluids are very sensitive to a moving boundary. This is probably due to weak intermolecular forces and even a small deformation of a boundary produces important modifications in a fluid flow. For this reason, it is necessary to write the fluid equations in a moving domain. Coupling Navier-Stokes equations with a linear model for the structure was used in [21], [11], [23], [2], [26] where the structure is governed by the independent rings or linear membrane model. In applications with large deformations of the structure, non-linear structure models have to be used as in [16], [14], [27], [10] (shells) or in [3] (beams). In a future work, we intend to replace the linear elasticity equations by a non-linear hyper-elastic model.*

## 3 Weak formulation of the model

Let $\mathbf{w}^F$ be a test function defined on $\Omega_t^F$, such that $\mathbf{w}^F = 0$ on $\Sigma_2$. Let us multiply the equation (1) by $\mathbf{w}^F$ and using the Green's formula, we get:

$$\int_{\Omega_t^F} \rho^F \left.\frac{\partial \mathbf{v}}{\partial t}\right|_{\widehat{\mathbf{x}}} \cdot \mathbf{w}^F + \int_{\Omega_t^F} \rho^F \left(\left(\left(\mathbf{v}-\boldsymbol{\vartheta}\right)\cdot\nabla\right)\mathbf{v}\right)\cdot\mathbf{w}^F$$
$$+ \int_{\Omega_t^F} 2\mu^F \epsilon\left(\mathbf{v}\right) : \epsilon\left(\mathbf{w}^F\right) - \int_{\Omega_t^F} \left(\nabla\cdot\mathbf{w}^F\right) p = \int_{\Omega_t^F} \mathbf{f}^F\cdot\mathbf{w}^F$$
$$+ \int_{\Gamma_t} \left(\sigma^F\mathbf{n}^F\right)\cdot\mathbf{w}^F + \int_{\Sigma_1} \mathbf{h}_{in}\cdot\mathbf{w}^F + \int_{\Sigma_3} \mathbf{h}_{out}\cdot\mathbf{w}^F. \tag{14}$$

Also, when we multiply the equation (7) by $\mathbf{w}^S : \Omega^S \longrightarrow \mathbb{R}^2$ such that $\mathbf{w}^S = 0$ on $\Gamma_D$, using again the Green's formula, we obtain:

$$\int_{\Omega^S} \rho^S \frac{\partial^2 \mathbf{u}}{\partial t^2}\cdot\mathbf{w}^S + a_S\left(\mathbf{u},\mathbf{w}^S\right) = \int_{\Omega^S}\mathbf{f}^S\cdot\mathbf{w}^S + \int_{\Gamma_0}\left(\sigma^S\mathbf{n}^S\right)\cdot\mathbf{w}^S, \tag{15}$$

where

$$a_S\left(\mathbf{u},\mathbf{w}^S\right) = \int_{\Omega^S}\lambda^S\left(\nabla\cdot\mathbf{u}\right)\left(\nabla\cdot\mathbf{w}^S\right) + \int_{\Omega^S} 2\mu^S\epsilon\left(\mathbf{u}\right):\epsilon\left(\mathbf{w}^S\right).$$

If $\mathbf{w}^S = \mathbf{w}^F\circ\mathbb{T}$ at the interface $\Gamma_0$ and from the equation (13), we have :

$$\int_{\Gamma_0}\left(\sigma^S\mathbf{n}^S\right)\cdot\mathbf{w}^S + \int_{\Gamma_t}\left(\sigma^F\mathbf{n}^F\right)\cdot\mathbf{w}^F = 0. \tag{16}$$

Now, if we multiply the equation (2) by $q \in L^2(\Omega_t^F)$, taking the sum with the precedent equations (14), (15) and referring to (16), we get the following weak formulation of (1)-(13): find $\mathbf{v} \in (H^1(\Omega_t^F))^2$, $\mathbf{v} = 0$ on $\Sigma_2\times[0,T]$, $p\in L^2(\Omega_t^F)$ and $\mathbf{u}\in(H^1(\Omega^S))^2$, $\mathbf{u}=0$ on $\Gamma_D$ with $\mathbf{v}(X+\mathbf{u}(X,t),t) = \frac{\partial\mathbf{u}}{\partial t}(X,t)$ on $\Gamma_0\times[0,T]$ solving:

$$\int_{\Omega_t^F} \rho^F \left.\frac{\partial \mathbf{v}}{\partial t}\right|_{\widehat{\mathbf{x}}} \cdot \mathbf{w}^F + \int_{\Omega_t^F} \rho^F \left(\left(\left(\mathbf{v}-\boldsymbol{\vartheta}\right)\cdot\nabla\right)\mathbf{v}\right)\cdot\mathbf{w}^F$$
$$+ \int_{\Omega_t^F} 2\mu^F \epsilon\left(\mathbf{v}\right) : \epsilon\left(\mathbf{w}^F\right) - \int_{\Omega_t^F}\left(\nabla\cdot\mathbf{w}^F\right)p - \int_{\Omega_t^F}\left(\nabla\cdot\mathbf{v}\right)q$$
$$+ \int_{\Omega^S}\rho^S\frac{\partial^2\mathbf{u}}{\partial t^2}\cdot\mathbf{w}^S + a_S\left(\mathbf{u},\mathbf{w}^S\right) = \int_{\Omega_t^F}\mathbf{f}^F\cdot\mathbf{w}^F + \int_{\Omega^S}\mathbf{f}^S\cdot\mathbf{w}^S$$
$$+ \int_{\Sigma_1}\mathbf{h}_{in}\cdot\mathbf{w}^F + \int_{\Sigma_3}\mathbf{h}_{out}\cdot\mathbf{w}^F, \tag{17}$$

for any $\mathbf{w}^F \in (H^1(\Omega_t^F))^2$; $\mathbf{w}^F = 0$ on $\Sigma_2 \times [0,T]$, $\mathbf{w}^S \in (H^1(\Omega^S))^2$; $\mathbf{w}^S = 0$ on $\Gamma_D$ with $\mathbf{w}^F(X + \mathbf{u}(X,t),t) = \dfrac{\partial \mathbf{w}^F}{\partial t}(X,t)$ on $\Gamma_0 \times [0,T]$ and for any $q \in L^2(\Omega_t^F)$.

## 4 Time discretization

Let $N \in \mathbb{N}^*$ be the number of time steps and we denote by $\Delta t = \dfrac{T}{N}$ the step time. We set $t_n = n\Delta t$ for $n = 0, \ldots, N$ the subdivision points of $[0,T]$. We suppose that $\mathbf{f}^F : [0,T] \longrightarrow (L^2(\Omega_t^F))^2$, $\mathbf{h}_{in} : [0,T] \longrightarrow L^2(\Sigma_1)$, $\mathbf{h}_{out} : [0,T] \longrightarrow L^2(\Sigma_3)$ and $\mathbf{f}^S : [0,T] \longrightarrow (L^2(\Omega^S))^2$ are continuous maps and we set $\mathbf{f}^n = \mathbf{f}^F(n\Delta t)$, $\mathbf{h}_{in}^n = \mathbf{h}_{in}(n\Delta t)$, $\mathbf{h}_{out}^n = \mathbf{h}_{out}(n\Delta t)$ and $\mathbf{g}^n = \mathbf{f}^S(n\Delta t)$. We define $\mathbf{u}^n$ the approximation of $\mathbf{u}(n\Delta t)$.

For the fluid equations, we consider an implicit Euler scheme for the time derivative and a linearization of the convection term. For the structure, we employ a $\theta$-centered scheme of second-order in time.

We set $\widehat{\Omega}^F = \Omega_n^F$ and we define $\boldsymbol{\vartheta}^n = (\vartheta_1^n, \vartheta_2^n)^T$ the velocity of the fluid domain as solution of:

$$\begin{cases} \Delta_{\widehat{\mathbf{x}}} \boldsymbol{\vartheta}^n = 0, & \Omega_n^F \\ \boldsymbol{\vartheta}^n = 0, & \partial\Omega_n^F \setminus \Gamma_n \\ \boldsymbol{\vartheta}^n = \mathbf{v}^n, & \Gamma_n, \end{cases} \tag{18}$$

where $\mathbf{v}^n$ is the fluid velocity at time $n$ on $\Omega_n^F$. Under the assumption that $\Omega_n^F$ is Lipschitz, we have $\boldsymbol{\vartheta}^n \in (H^1(\Omega_n^F))^2$.

For all $n = 0, \cdots, N-1$, we denote by $\mathcal{A}_{t_{n+1}}$ the map from $\overline{\Omega}_n^F$ in $\mathbb{R}^2$ defined by:

$$\begin{aligned}\mathcal{A}_{t_{n+1}}(\widehat{x}_1,\widehat{x}_2) : \overline{\Omega}_n^F &\longrightarrow \mathbb{R}^2\\ (\widehat{x}_1,\widehat{x}_2) &\mapsto (\widehat{x}_1+\Delta t\vartheta_1^n, \widehat{x}_2+\Delta t\vartheta_2^n).\end{aligned}$$

We set $\Omega_{n+1}^F = \mathcal{A}_{t_{n+1}}(\Omega_n^F)$ and $\Gamma_{n+1} = \mathcal{A}_{t_{n+1}}(\Gamma_n)$. We define the following map: $\mathbb{T} = \mathcal{A}_{t_n} \circ \mathcal{A}_{t_{n-1}} \cdots \circ \mathcal{A}_{t_1}$ and we may observe that $\Gamma_n = \mathbb{T}(\Gamma_0)$.

The Jacobian of $\mathcal{A}_{t_{n+1}}$ is obtained by:

$$1+\Delta t(\nabla_{\widehat{\mathbf{x}}}\cdot\boldsymbol{\vartheta}^n)+(\Delta t)^2\Big(\frac{\partial\vartheta_1^n}{\partial\widehat{x}_1}\cdot\frac{\partial\vartheta_2^n}{\partial\widehat{x}_2}-\frac{\partial\vartheta_2^n}{\partial\widehat{x}_1}\cdot\frac{\partial\vartheta_1^n}{\partial\widehat{x}_2}\Big).$$

We need again to define the following test function spaces :

$$\begin{aligned}\widehat{W}_n^F &= \{\widehat{\mathbf{w}}^F \in (H^1(\Omega_n^F))^2;\ \widehat{\mathbf{w}}^F = 0 \text{ on } \Sigma_2\}\\ \widehat{Q}_n^F &= L^2(\Omega_n^F)\\ W^S &= \{\mathbf{w}^S \in (H^1(\Omega^S))^2;\ \mathbf{w}^S = 0 \text{ on } \Gamma_D\}.\end{aligned}$$

We assume that we know $\Omega_n^F$, $\mathbf{v}^n \in (L^2(\Omega_n^F))^2$, $\mathbf{u}^{n-1}, \mathbf{u}^n \in \Big(L^2(\Omega^S)\Big)^2$.

**Step** 1: Find $\boldsymbol{\vartheta}^n \in (H^1(\Omega_n^F))^2$ solution of the system (18)

**Step** 2: Find $\widehat{\mathbf{v}}^{n+1} \in \widehat{W}_n^F$, $\widehat{p}^{n+1} \in \widehat{Q}_n^F$, $\mathbf{u}^{n+1} \in W^S$ with

$$\widehat{\mathbf{v}}^{n+1}\circ\mathbb{T} = \frac{\mathbf{u}^{n+1}-\mathbf{u}^{n-1}}{2\Delta t}, \quad \text{on } \Gamma_0$$

such that:

$$
\begin{aligned}
&\rho^F \int_{\Omega_n^F} \frac{(\widehat{\mathbf{v}}^{n+1} - \mathbf{v}^n)}{\Delta t} \cdot \widehat{\mathbf{w}}^F + \rho^F \int_{\Omega_n^F} (((\mathbf{v}^n - \boldsymbol{\vartheta}^n) \cdot \nabla_{\widehat{\mathbf{x}}}) \widehat{\mathbf{v}}^{n+1}) \cdot \widehat{\mathbf{w}}^F \\
&+ \frac{\rho^F}{2} \int_{\Omega_n^F} \delta(\widehat{\mathbf{x}}) \widehat{\mathbf{v}}^{n+1} \cdot \widehat{\mathbf{w}}^F + 2\mu^F \int_{\Omega_n^F} \epsilon_{\widehat{\mathbf{x}}}(\widehat{\mathbf{v}}^{n+1}) : \epsilon_{\widehat{\mathbf{x}}}(\widehat{\mathbf{w}}^F) \\
&- \int_{\Omega_n^F} \widehat{p}^{n+1} (\nabla_{\widehat{\mathbf{x}}} \cdot \widehat{\mathbf{w}}^F) - \int_{\Omega_n^F} \widehat{q} (\nabla_{\widehat{\mathbf{x}}} \cdot \widehat{\mathbf{v}}^{n+1}) \\
&+ \rho^S \int_{\Omega^S} \Big( \frac{\mathbf{u}^{n+1} - 2\mathbf{u}^n + \mathbf{u}^{n-1}}{\Delta t^2} \Big) \cdot \mathbf{w}^S \\
&+ a_S(\theta \mathbf{u}^{n+1} + (1-2\theta)\mathbf{u}^n + \theta \mathbf{u}^{n-1}, \mathbf{w}^S) \\
&= \int_{\Omega_n^F} \widehat{\mathbf{f}}^{n+1} \cdot \widehat{\mathbf{w}}^F + \int_{\Omega^S} \overline{\mathbf{g}}^{n+1} \cdot \mathbf{w}^S + \int_{\Sigma_1} \mathbf{h}_{in}^{n+1} \cdot \widehat{\mathbf{w}}^F + \int_{\Sigma_3} \mathbf{h}_{out}^{n+1} \cdot \widehat{\mathbf{w}}^F, \qquad (19)
\end{aligned}
$$

for any $\widehat{\mathbf{w}}^F \in \widehat{W}_n,\ \widehat{q} \in \widehat{Q}_n^F,\ \mathbf{w}^S \in W^S$ with $\mathbf{w}^S = \widehat{\mathbf{w}}^F \circ \mathbb{T}$ on $\Gamma_0$,

where

$$
\widehat{\mathbf{f}}^{n+1} = \mathbf{f}^{n+1} \circ \mathcal{A}_{t_{n+1}} \text{ et } \overline{\mathbf{g}}^{n+1} = \theta \mathbf{g}^{n+1} + (1-2\theta)\mathbf{g}^n + \theta \mathbf{g}^{n-1}
$$

and

$$
\delta(\widehat{\mathbf{x}}) = \Delta t \Big( \frac{\partial \vartheta_1^n}{\partial \widehat{x}_1} \cdot \frac{\partial \vartheta_2^n}{\partial \widehat{x}_2} - \frac{\partial \vartheta_2^n}{\partial \widehat{x}_1} \cdot \frac{\partial \vartheta_1^n}{\partial \widehat{x}_2} \Big).
$$

**Remark 2** *Let us explain why the first term of the second line in (19) was added. First, this term contains $\Delta t$, therefore the scheme does not lose consistency after adding this term. The term containing $\delta(\widehat{\mathbf{x}})$ was added in order to obtain the stability without supplementary condition on the mesh velocity. We will see in the next section where the stability is proved that, adding the term containing $\delta(\widehat{\mathbf{x}})$ allows us to obtain the exact expression of the Jacobian of the map $\mathcal{A}_{t_{n+1}}$ and then, the integral over $\Omega_n^F$ of the terms containing the mesh velocity can be rewritten as an integral over $\Omega_{n+1}^F$. In this way, the mesh velocity will be eliminated from the a-priori estimate. In fact, the mesh velocity is hidden in the definition of $\Omega_{n+1}^F$.*

The system (19) can be reformulated as following :

$$\rho^F \int_{\Omega_n^F} \Big[\frac{\widehat{\mathbf{v}}^{n+1}}{\Delta t} + ((\mathbf{v}^n - \boldsymbol{\vartheta}^n)\cdot\nabla_{\widehat{\mathbf{x}}})\widehat{\mathbf{v}}^{n+1} + \frac{1}{2}\delta(\widehat{\mathbf{x}})\widehat{\mathbf{v}}^{n+1}\Big]\cdot\widehat{\mathbf{w}}^F$$
$$+a_F(\widehat{\mathbf{v}}^{n+1},\widehat{\mathbf{w}}^F) + b_F(\widehat{\mathbf{w}}^F,\widehat{p}^{n+1}) + b_F(\widehat{\mathbf{v}}^{n+1},\widehat{q})$$
$$+\rho^S \int_{\Omega^S}\Big(\frac{\mathbf{u}^{n+1}-2\mathbf{u}^n+\mathbf{u}^{n-1}}{\Delta t^2}\Big)\cdot\mathbf{w}^S$$
$$+a_S(\theta\mathbf{u}^{n+1}+(1-2\theta)\mathbf{u}^n+\theta\mathbf{u}^{n-1},\mathbf{w}^S) = \rho^F\int_{\Omega_n^F}\frac{\mathbf{v}^n}{\Delta t}\cdot\widehat{\mathbf{w}}^F$$
$$+\int_{\Omega_n^F}\widehat{\mathbf{f}}^{n+1}\cdot\widehat{\mathbf{w}}^F + \int_{\Omega^S}\overline{\mathbf{g}}^{n+1}\cdot\mathbf{w}^S + \int_{\Sigma_1}\mathbf{h}_{in}^{n+1}\cdot\widehat{\mathbf{w}}^F + \int_{\Sigma_3}\mathbf{h}_{out}^{n+1}\cdot\widehat{\mathbf{w}}^F \qquad (20)$$

for all $\widehat{\mathbf{w}}^F \in \widehat{W}_n^F$, $\mathbf{w}^S \in W^S$ with $\mathbf{w}^S = \widehat{\mathbf{w}}^F \circ \mathbb{T}$ on $\Gamma_0$ and $\widehat{q} \in \widehat{Q}_n^F$, where

$$a_F(\widehat{\mathbf{v}},\widehat{\mathbf{w}}^F) = 2\mu^F\int_{\Omega_n^F}\epsilon(\widehat{\mathbf{v}}):\epsilon(\widehat{\mathbf{w}}^F) \quad \text{and} \quad b_F(\widehat{\mathbf{w}}^F,\widehat{q}) = -\int_{\Omega_n^F}\widehat{q}(\nabla\cdot\widehat{\mathbf{w}}^F).$$

## 5 Stability

We denote by

$$X^n = \theta a_S(\mathbf{u}^n,\mathbf{u}^n) + (1-2\theta)a_S(\mathbf{u}^n,\mathbf{u}^{n-1}) + \theta a_S(\mathbf{u}^{n-1},\mathbf{u}^{n-1}) \qquad (21)$$

and we define $\mathbf{v}^{n+1}$ to be the fluid velocity at time $(n+1)$ by:

$$\mathbf{v}^{n+1}(\mathbf{x}) = \widehat{\mathbf{v}}^{n+1}(\widehat{\mathbf{x}}), \quad \forall\,\mathbf{x}\in\Omega_{n+1}^F,\ \forall\,\widehat{\mathbf{x}}\in\Omega_n^F,\ \text{with } \mathbf{x} = \widehat{\mathbf{x}} + \Delta t\boldsymbol{\vartheta}^n(\widehat{\mathbf{x}}).$$

We have the following stability result:

**Theorem 1** *Let $\Omega_n^F$ be a bounded domain of $\mathbb{R}^2$. We suppose that $\int_{\Sigma_1\cup\Sigma_3}(\mathbf{v}^n\cdot\mathbf{n}^F)|\widehat{\mathbf{v}}^{n+1}|^2 \geq 0$. Then the following energy estimation holds:*

$$\rho^F\|\mathbf{v}^{n+1}\|^2_{L^2(\Omega^F_{n+1})}+2\mu^F\Delta t\|\epsilon_{\widehat{\mathbf{x}}}(\widehat{\mathbf{v}}^{n+1})\|^2_{L^2(\Omega^F_n)}+\rho^S\left\|\frac{\mathbf{u}^{n+1}-\mathbf{u}^n}{\Delta t}\right\|^2_{L^2(\Omega^S)}$$
$$+X^{n+1}\leq\exp(T)\Big[\rho^F\|\mathbf{v}^1\|^2_{L^2(\Omega^F_1)}+2\mu^F\Delta t\|\epsilon_{\widehat{\mathbf{x}}}(\widehat{\mathbf{v}}^1)\|^2_{L^2(\Omega^F_0)}$$
$$+\rho^S\left\|\frac{\mathbf{u}^1-\mathbf{u}^0}{\Delta t}\right\|^2_{L^2(\Omega^S)}+X^1+C\Big(\max_{t\in[0,T]}\|\mathbf{f}^F(t)\|^2_{L^2(\Omega^F_t)}$$
$$+\max_{t\in[0,T]}\|\mathbf{f}^S(t)\|^2_{L^2(\Omega^S)}+\max_{t\in[0,T]}\|\mathbf{h}_{in}(t)\|^2_{L^2(\Sigma_1)}+\max_{t\in[0,T]}\|\mathbf{h}_{out}(t)\|^2_{L^2(\Sigma_3)}\Big)\Big],$$

*where $C>0$ is independent of $\Delta t$.*
*If furthermore, $\theta\in\left[\frac{1}{4},\frac{1}{2}\right]$, then:*

$$\|\mathbf{v}^{n+1}\|_{L^2(\Omega^F_{n+1})},\ \ \Delta t\|\epsilon_{\widehat{\mathbf{x}}}(\widehat{\mathbf{v}}^{n+1})\|_{L^2(\Omega^F_n)},\ \ \left\|\frac{\mathbf{u}^{n+1}-\mathbf{u}^n}{\Delta t}\right\|_{L^2(\Omega^S)}\ \textit{and}\ X^{n+1}$$

*are bounded.*

Before starting the proof of the stability theorem, we need to show some lemmas.

We denote by

$$c_F(\widehat{\mathbf{v}}^{n+1},\widehat{\mathbf{w}}^F)=\rho^F\int_{\Omega^F_n}\left[\frac{\widehat{\mathbf{v}}^{n+1}}{\Delta t}+((\mathbf{v}^n-\boldsymbol{\vartheta}^n)\cdot\nabla_{\widehat{\mathbf{x}}})\widehat{\mathbf{v}}^{n+1}+\frac{1}{2}\delta(\widehat{\mathbf{x}})\widehat{\mathbf{v}}^{n+1}\right]\cdot\widehat{\mathbf{w}}^F.$$

**Lemma 1** *The following inequality holds*

$$2\Delta t c_F(\widehat{\mathbf{v}}^{n+1},\widehat{\mathbf{v}}^{n+1})\geq\rho^F\|\widehat{\mathbf{v}}^{n+1}\|^2_{L^2(\Omega^F_n)}+\rho^F\|\mathbf{v}^{n+1}\|^2_{L^2(\Omega^F_{n+1})}.$$

**Proof.** Let us set $|\widehat{\mathbf{v}}^{n+1}|^2=(\widehat{\mathrm{v}}_1^{n+1})^2+(\widehat{\mathrm{v}}_2^{n+1})^2$, then we have:

$$2\Delta t c_F(\widehat{\mathbf{v}}^{n+1},\widehat{\mathbf{v}}^{n+1})$$
$$=2\Delta t\rho^F\int_{\Omega^F_n}\left[\frac{\widehat{\mathbf{v}}^{n+1}}{\Delta t}+((\mathbf{v}^n-\boldsymbol{\vartheta}^n)\cdot\nabla_{\widehat{\mathbf{x}}})\widehat{\mathbf{v}}^{n+1}+\frac{1}{2}\delta(\widehat{\mathbf{x}})\widehat{\mathbf{v}}^{n+1}\right]\cdot\widehat{\mathbf{v}}^{n+1}$$
$$=2\rho^F\int_{\Omega^F_n}|\widehat{\mathbf{v}}^{n+1}|^2+2\Delta t\rho^F\int_{\Omega^F_n}\left[((\mathbf{v}^n-\boldsymbol{\vartheta}^n)\cdot\nabla_{\widehat{\mathbf{x}}})\widehat{\mathbf{v}}^{n+1}\right]\cdot\widehat{\mathbf{v}}^{n+1}$$
$$+\rho^F\Delta t\int_{\Omega^F_n}\delta(\widehat{\mathbf{x}})|\widehat{\mathbf{v}}^{n+1}|^2.$$

The middle term of the previous expression can be written as

$$2\Delta t\rho^F \int_{\Omega_n^F} \left[((\mathbf{v}^n - \boldsymbol{\vartheta}^n)\cdot\nabla_{\widehat{\mathbf{x}}})\widehat{\mathbf{v}}^{n+1}\right]\cdot\widehat{\mathbf{v}}^{n+1} = \rho^F\Delta t\int_{\Omega_n^F}(\mathbf{v}^n-\boldsymbol{\vartheta}^n)\cdot\nabla_{\widehat{\mathbf{x}}}(|\widehat{\mathbf{v}}^{n+1}|^2).$$

Now, when we integrate it by part we obtain :

$$\begin{aligned}&\rho^F\Delta t\int_{\Omega_n^F}(\mathbf{v}^n-\boldsymbol{\vartheta}^n)\cdot\nabla_{\widehat{\mathbf{x}}}(|\widehat{\mathbf{v}}^{n+1}|^2) = -\rho^F\Delta t\int_{\Omega_n^F}\nabla_{\widehat{\mathbf{x}}}\cdot(\mathbf{v}^n-\boldsymbol{\vartheta}^n)|\widehat{\mathbf{v}}^{n+1}|^2\\ &+\rho^F\Delta t\int_{\partial\Omega_n^F}\Big((\mathbf{v}^n-\boldsymbol{\vartheta}^n)\cdot\mathbf{n}^F\Big)|\widehat{\mathbf{v}}^{n+1}|^2.\end{aligned}$$

For the boundary term, we have $\rho^F\Delta t\int_{\partial\Omega_n^F}\Big((\mathbf{v}^n-\boldsymbol{\vartheta}^n)\cdot\mathbf{n}^F\Big)|\widehat{\mathbf{v}}^{n+1}|^2\geq 0$, in fact it vanishes on $\Gamma_n$ since $\mathbf{v}^n=\boldsymbol{\vartheta}^n$, it vanishes again on $\Sigma_2$ since $\widehat{\mathbf{v}}^{n+1}=0$. On $\Sigma_1\cup\Sigma_3$, we have $\boldsymbol{\vartheta}^n=0$ and $\int_{\Sigma_1\cup\Sigma_3}(\mathbf{v}^n\cdot\mathbf{n}^F)|\widehat{\mathbf{v}}^{n+1}|^2$ is supposed to be positive. Using now the assumption that $\nabla_{\widehat{\mathbf{x}}}\cdot\mathbf{v}^n=0$, we get

$$-\rho^F\Delta t\int_{\Omega_n^F}\nabla_{\widehat{\mathbf{x}}}\cdot(\mathbf{v}^n-\boldsymbol{\vartheta}^n)|\widehat{\mathbf{v}}^{n+1}|^2 = \rho^F\Delta t\int_{\Omega_n^F}(\nabla_{\widehat{\mathbf{x}}}\cdot\boldsymbol{\vartheta}^n)|\widehat{\mathbf{v}}^{n+1}|^2.$$

This implies that

$$\begin{aligned}2\rho^F\Delta t c_F(\widehat{\mathbf{v}}^{n+1},\widehat{\mathbf{v}}^{n+1}) \geq\ & 2\rho^F\|\widehat{\mathbf{v}}^{n+1}\|^2_{L^2(\Omega_n^F)}\\ &+\rho^F\int_{\Omega_n^F}\Big(\Delta t(\nabla_{\widehat{\mathbf{x}}}\cdot\boldsymbol{\vartheta}^n)+\delta(\widehat{\mathbf{x}})\Delta t\Big)|\widehat{\mathbf{v}}^{n+1}|^2.\end{aligned}$$

If we add and subtract $\rho^F\int_{\Omega_n^F}|\widehat{\mathbf{v}}^{n+1}|^2$ in the second member of the above inequality, we have:

$$\begin{aligned}2\rho^F\Delta t c_F(\widehat{\mathbf{v}}^{n+1},\widehat{\mathbf{v}}^{n+1}) \geq\ & \rho^F\|\widehat{\mathbf{v}}^{n+1}\|^2_{L^2(\Omega_n^F)}\\ &+\rho^F\int_{\Omega_n^F}\Big(1+\Delta t(\nabla_{\widehat{\mathbf{x}}}\cdot\boldsymbol{\vartheta}^n)+\delta(\widehat{\mathbf{x}})\Delta t\Big)|\widehat{\mathbf{v}}^{n+1}|^2.\end{aligned}$$

We recalled at the beginning that $\Big(1+\Delta t(\nabla_{\widehat{\mathbf{x}}}\cdot\boldsymbol{\vartheta}^n)+\Delta t\delta(\widehat{\mathbf{x}})\Big)$ is the Jacobian of $\mathcal{A}_{t_{n+1}}$ and by changing the domain, under the assumption that $\mathbf{v}^{n+1}\in$

$(L^2(\Omega^F_{n+1}))^2$, we have:

$$\rho^F \int_{\Omega^F_n} \Big(1 + \Delta t(\nabla_{\widehat{\mathbf{x}}} \cdot \boldsymbol{\vartheta}^n) + \delta(\widehat{\mathbf{x}})\Delta t\Big)|\widehat{\mathbf{v}}^{n+1}|^2 = \rho^F \int_{\Omega^F_{n+1}} |\mathbf{v}^{n+1}|^2.$$

Finally, we get:

$$2\rho^F \Delta t c_F(\widehat{\mathbf{v}}^{n+1}, \widehat{\mathbf{v}}^{n+1}) \geq \rho^F \|\widehat{\mathbf{v}}^{n+1}\|^2_{L^2(\Omega^F_n)} + \rho^F \|\mathbf{v}^{n+1}\|^2_{L^2(\Omega^F_{n+1})}.$$

■

**Remark 3** The following equality holds:

$$a_F(\widehat{\mathbf{v}}^{n+1}, 2\Delta t\widehat{\mathbf{v}}^{n+1}) = 4\mu^F \Delta t \|\epsilon_{\widehat{\mathbf{x}}}(\widehat{\mathbf{v}}^{n+1})\|^2_{L^2(\Omega^F_n)}.$$

In fact, by definition of $a_F(\cdot,\ \cdot)$ we have

$$\begin{aligned} &a_F(\widehat{\mathbf{v}}^{n+1}, 2\Delta t\widehat{\mathbf{v}}^{n+1}) = 4\mu^F \Delta t \int_{\Omega^F_n} \epsilon_{\widehat{\mathbf{x}}}(\widehat{\mathbf{v}}^{n+1}) : \epsilon_{\widehat{\mathbf{x}}}(\widehat{\mathbf{v}}^{n+1}) \\ &= 4\mu^F \Delta t \|\epsilon_{\widehat{\mathbf{x}}}(\widehat{\mathbf{v}}^{n+1})\|^2_{L^2(\Omega^F_n)}. \end{aligned}$$

**Remark 4** To compute the terms $b_F(\cdot,\ \cdot)$ in (20), we set $\widehat{\mathbf{w}}^F = 2\Delta t\widehat{\mathbf{v}}^{n+1}$ and $\widehat{q} = -2\Delta t\widehat{p}^{n+1}$, we get therefore :

$$b_F(\widehat{\mathbf{v}}^{n+1}, \widehat{q}) + b_F(\widehat{\mathbf{w}}^F, \widehat{p}^{n+1}) = 2\Delta t\Big( - b_F(\widehat{\mathbf{v}}^{n+1}, \widehat{p}^{n+1}) + b_F(\hat{\mathrm{v}}^{n+1}, \widehat{p}^{n+1})\Big) = 0.$$

**Lemma 2** *The following equality holds*

$$\begin{aligned} &\rho^S \int_{\Omega^S} \Big(\frac{\mathbf{u}^{n+1} - 2\mathbf{u}^n + \mathbf{u}^{n-1}}{(\Delta t)^2}\Big) \cdot (\mathbf{u}^{n+1} - \mathbf{u}^{n-1}) = \rho^S \Big\| \frac{\mathbf{u}^{n+1} - \mathbf{u}^n}{\Delta t} \Big\|^2_{L^2(\Omega^S)} \\ &-\rho^S \Big\| \frac{\mathbf{u}^n - \mathbf{u}^{n-1}}{\Delta t} \Big\|^2_{L^2(\Omega^S)}. \end{aligned}$$

**Proof.** Adding and substracting $\mathbf{u}^n$ to the term $(\mathbf{u}^{n+1} - \mathbf{u}^{n-1})$, we have :

$$\rho^S \int_{\Omega^S} \Big( \frac{\mathbf{u}^{n+1} - 2\mathbf{u}^n + \mathbf{u}^{n-1}}{(\Delta t)^2} \Big) \cdot (\mathbf{u}^{n+1} - \mathbf{u}^{n-1})$$
$$= \rho^S \int_{\Omega^S} \Big( \frac{\mathbf{u}^{n+1} - \mathbf{u}^n - (\mathbf{u}^n - \mathbf{u}^{n-1})}{(\Delta t)^2} \Big) \cdot (\mathbf{u}^{n+1} - \mathbf{u}^n + \mathbf{u}^n - \mathbf{u}^{n-1}).$$

Let us remark that the above expression can be identified as $(a+b)(a-b)$, thus

$$\rho^S \int_{\Omega^S} \Big( \frac{\mathbf{u}^{n+1} - 2\mathbf{u}^n + \mathbf{u}^{n-1}}{(\Delta t)^2} \Big) \cdot (\mathbf{u}^{n+1} - \mathbf{u}^{n-1}) = \rho^S \Big\| \frac{\mathbf{u}^{n+1} - \mathbf{u}^n}{\Delta t} \Big\|^2_{L^2(\Omega^S)}$$
$$-\rho^S \Big\| \frac{\mathbf{u}^n - \mathbf{u}^{n-1}}{\Delta t} \Big\|^2_{L^2(\Omega^S)}.$$

■

**Lemma 3** *We have*

$$a_S(\theta \mathbf{u}^{n+1} + (1-2\theta)\mathbf{u}^n + \theta \mathbf{u}^{n-1}, \mathbf{u}^{n+1} - \mathbf{u}^{n-1}) = X^{n+1} - X^n.$$

**Proof.** By bilinearity of the $a_S(\cdot,\ \cdot)$, we get

$$a_S(\theta \mathbf{u}^{n+1} + (1-2\theta)\mathbf{u}^n + \theta \mathbf{u}^{n-1}, \mathbf{u}^{n+1} - \mathbf{u}^{n-1})$$
$$= a_S(\theta \mathbf{u}^{n+1} + (1-2\theta)\mathbf{u}^n + \theta \mathbf{u}^{n-1}, \mathbf{u}^{n+1})$$
$$-a_S(\theta \mathbf{u}^{n+1} + (1-2\theta)\mathbf{u}^n + \theta \mathbf{u}^{n-1}, \mathbf{u}^n)$$
$$= \theta a_S(\mathbf{u}^{n+1}, \mathbf{u}^{n+1}) + (1-2\theta) a_S(\mathbf{u}^n, \mathbf{u}^{n+1}) + \theta a_S(\mathbf{u}^{n-1}, \mathbf{u}^{n+1})$$
$$-\theta a_S(\mathbf{u}^{n+1}, \mathbf{u}^{n-1}) - (1-2\theta) a_S(\mathbf{u}^n, \mathbf{u}^{n-1}) - \theta a_S(\mathbf{u}^{n-1}, \mathbf{u}^{n-1}).$$

Since $a_S(\cdot,\ \cdot)$ is symmetric, therefore $\theta a_S(\mathbf{u}^{n-1}, \mathbf{u}^{n+1}) - \theta a_S(\mathbf{u}^{n+1}, \mathbf{u}^{n-1}) = 0$. Moreover when we add and we substracte the term $\theta a_S(\mathbf{u}^n, \mathbf{u}^n)$ in the above final expression, we have:

$$a_S(\theta \mathbf{u}^{n+1} + (1-2\theta)\mathbf{u}^n + \theta \mathbf{u}^{n-1}, \mathbf{u}^{n+1} - \mathbf{u}^{n-1})$$
$$= \theta a_S(\mathbf{u}^{n+1}, \mathbf{u}^{n+1}) + (1-2\theta) a_S(\mathbf{u}^{n+1}, \mathbf{u}^n) + \theta a_S(\mathbf{u}^n, \mathbf{u}^n)$$
$$-\theta a_S(\mathbf{u}^n, \mathbf{u}^n) - (1-2\theta) a_S(\mathbf{u}^n, \mathbf{u}^{n-1}) - \theta a_S(\mathbf{u}^{n-1}, \mathbf{u}^{n-1}).$$

Hence, we obtain

$$a_S(\theta\mathbf{u}^{n+1} + (1-2\theta)\mathbf{u}^n + \theta\mathbf{u}^{n-1}, \mathbf{u}^{n+1} - \mathbf{u}^{n-1}) = X^{n+1} - X^n.$$

■

**Lemma 4** *There exist two constants $C_2 > 0$ and $C' > 0$ such that :*

$$\begin{aligned}
&\int_{\Omega_n^F} \widehat{\mathbf{f}}^{n+1} \cdot (2\Delta t\widehat{\mathbf{v}}^{n+1}) + \int_{\Sigma_1} \mathbf{h}_{in}^{n+1} \cdot (2\Delta t\widehat{\mathbf{v}}^{n+1}) + \int_{\Sigma_3} \mathbf{h}_{out}^{n+1} \cdot (2\Delta t\widehat{\mathbf{v}}^{n+1}) \\
&\leq \Delta t\Big(C_2\|\widehat{\mathbf{f}}^{n+1}\|^2_{L^2(\Omega_n^F)} + C'\|\mathbf{h}_{int}^{n+1}\|^2_{L^2(\Sigma_1)} + C'\|\mathbf{h}_{out}^{n+1}\|^2_{L^2(\Sigma_3)}\Big) \\
&+2\mu^F\Delta t\|\epsilon_{\widehat{\mathbf{x}}}(\widehat{\mathbf{v}}^{n+1})\|^2_{L^2(\Omega_n^F)}.
\end{aligned}$$

Before starting the proof of the Lemma 4, we recall two functional analysis lemmas.

**Lemma 5 (Korn lemma, see [7], page 123)** *Let $\Omega$ be a convex and bounded open subset of $\mathbb{R}^n$. We denote by $V$ the subspace of $(H^1(\Omega))^n$ defined by $V = \Big\{v \in (H^1(\Omega))^n; \quad v\Big|_\Gamma = 0\Big\}$, where $\Gamma$ is a part of the boundary $\partial\Omega$ with $mes(\Gamma) > 0$. Then, there exists a constant $C_\Omega$ such that:*

$$\|v\|^2_{L^2(\Omega)} \leq C_\Omega\|\epsilon(v)\|^2_{L^2(\Omega)}, \quad \forall\ v \in V.$$

**Lemma 6 (Trace theorem, see [24], page 10)** *Let $\Omega$ be a bounded open subset of $\mathbb{R}^n$, with Lipschitz continuous boundary $\partial\Omega$. We define the trace map by:*

$$\begin{aligned}
\gamma_0 :\ H^1(\Omega) \cap C(\overline{\Omega}) &\longrightarrow L^2(\partial\Omega) \cap C(\overline{\partial\Omega}) \\
v &\mapsto \gamma_0(v) = v\Big|_{\partial\Omega}
\end{aligned}$$

*This map $\gamma_0$ can be extended by continuity to the linear continuous map from $H^1(\Omega)$ to $L^2(\partial\Omega)$, also called $\gamma_0$. In particular there exists a constant $C_{\gamma_0} > 0$*

*such that for all* $v \in H^1(\Omega)$

$$\|v\|_{L^2(\partial\Omega)} \leq C_{\gamma_0}\|v\|_{H^1(\Omega)}.$$

**Proof. (Lemme 4)** First, let us set $A = \displaystyle\int_{\Omega_n^F} \widehat{\mathbf{f}}^{n+1} \cdot (2\Delta t)\widehat{\mathrm{v}}^{n+1}$ and by the Cauchy-Schwarz' inequality, we get

$$A \leq 2\Delta t\|\widehat{\mathbf{f}}^{n+1}\|_{L^2(\Omega_n^F)}\|\widehat{\mathbf{v}}^{n+1}\|_{L^2(\Omega_n^F)}.$$

We have from Lemma 5, that there exists a constant $C_{\Omega_n^F} > 0$ (we after take $C_1 = 2\sqrt{C_{\Omega_n^F}}$) such that:

$$A \leq C_1\Delta t\|\widehat{\mathbf{f}}^{n+1}\|_{L^2(\Omega_n^F)}\|\epsilon_{\widehat{\mathbf{x}}}(\widehat{\mathbf{v}}^{n+1})\|_{L^2(\Omega_n^F)}.$$

Setting

$$a = \frac{C_1\|\widehat{\mathbf{f}}^{n+1}\|_{L^2(\Omega_n^F)}}{\sqrt{2\mu^F}}, \quad b = \sqrt{2\mu^F}\|\epsilon_{\widehat{\mathbf{x}}}(\widehat{\mathbf{v}}^{n+1})\|_{L^2(\Omega_n^F)}$$

and using the following Young's inequality:

$$ab \leq \frac{a^2}{2} + \frac{b^2}{2}, \ \ \forall\, a, b \geq 0, \tag{22}$$

we finally obtain that there exists a $C_2 = \dfrac{C_1^2}{4\mu^F} > 0$ such that:

$$A \leq C_2\Delta t\|\widehat{\mathbf{f}}^{n+1}\|^2_{L^2(\Omega_n^F)} + \mu^F\Delta t\|\epsilon_{\widehat{\mathbf{x}}}(\widehat{\mathbf{v}}^{n+1})\|^2_{L^2(\Omega_n^F)}.$$

Second, let us set

$$B = \int_{\Sigma_1} \mathbf{h}_{in}^{n+1} \cdot (2\Delta t)\mathbf{v}^{n+1} + \int_{\Sigma_3} \mathbf{h}_{out}^{n+1} \cdot (2\Delta t)\mathbf{v}^{n+1}.$$

From Cauchy-Schwarz' inequality, we have

$$B \leq 2\Delta t\Big(\|\mathbf{h}_{in}^{n+1}\|_{L^2(\Sigma_1)} + \|\mathbf{h}_{out}^{n+1}\|_{L^2(\Sigma_3)}\Big)\|\gamma_0(\widehat{\mathbf{v}}^{n+1})\|_{L^2(\partial\Omega_n^F)}$$

and referring to the Lemma 6, there exists a constant $C_{\gamma_0} > 0$ (we after take $C_3 = 2C_{\gamma_0}$) such that

$$B \leq \Delta t C_3 \Big( \|\mathbf{h}_{in}^{n+1}\|_{L^2(\Sigma_1)} + \|\mathbf{h}_{out}^{n+1}\|_{L^2(\Sigma_3)} \Big) \|\widehat{\mathbf{v}}^{n+1}\|_{H^1(\Omega_n^F)}.$$

We set

$$a = C_3 \sqrt{\frac{1 + C_{\Omega_n^F}}{2\mu^F}} \Big( \|\mathbf{h}_{in}^{n+1}\|_{L^2(\Sigma_1)} + \|\mathbf{h}_{out}^{n+1}\|_{L^2(\Sigma_3)} \Big)$$

and

$$b = \sqrt{\frac{2\mu^F}{1 + C_{\Omega_n^F}}} \|\mathbf{v}^{n+1}\|_{H^1(\Omega_n^F)}.$$

Using (22) and Lemma 5 ($\|\widehat{\mathbf{v}}^{n+1}\|^2_{H^1(\Omega_n^F)} \leq (1 + C_{\Omega_n^F}) \|\epsilon_{\widehat{x}}(\widehat{\mathbf{v}}^{n+1})\|^2_{L^(\Omega_n^F)}$), we get

$$B \leq C_4 \Delta t \Big( \|\mathbf{h}_{in}^{n+1}\|_{L^2(\Sigma_1)} + \|\mathbf{h}_{out}^{n+1}\|_{L^2(\Sigma_3)} \Big)^2 + \mu^F \Delta t \|\epsilon_{\widehat{x}}(\widehat{\mathbf{v}}^{n+1})\|^2_{L^(\Omega_n^F)}.$$

By the inequality $(a+b)^2 \leq 2(a^2 + b^2)$, there exists a constant $C' = 2C_4$ such that

$$B \leq \Delta t C' \Big( \|\mathbf{h}_{in}^{n+1}\|^2_{L^2(\Sigma_1)} + \|\mathbf{h}_{out}^{n+1}\|^2_{L^2(\Sigma_3)} \Big) + \mu^F \Delta t \|\epsilon_{\widehat{x}}(\widehat{\mathbf{v}}^{n+1})\|^2_{L^(\Omega_n^F)}$$

Finally, taking the sum of $A$ and $B$ we get the lemma. ■

**Lemma 7** *The following inequality holds*

$$\rho^F \int_{\Omega_n^F} \frac{\mathbf{v}^n}{\Delta t} \cdot (2\Delta t \widehat{\mathbf{v}}^{n+1}) \leq \rho^F \|\mathbf{v}^n\|^2_{L^2(\Omega_n^F)} + \rho^F \|\widehat{\mathbf{v}}^{n+1}\|^2_{L^2(\Omega_n^F)}.$$

**Proof.** We have

$$\rho^F \int_{\Omega_n^F} \frac{\mathbf{v}^n}{\Delta t} \cdot (2\Delta t \widehat{\mathbf{v}}^{n+1}) = 2\rho^F \int_{\Omega_n^F} \mathbf{v}^n \cdot \widehat{\mathbf{v}}^{n+1} \leq 2\rho^F \|\mathbf{v}^n\|_{L^2(\Omega_n^F)} \|\widehat{\mathbf{v}}^{n+1}\|_{L^2(\Omega_n^F)},$$

and from (22) (with $a = \|\mathbf{v}^n\|_{L^2(\Omega_n^F)}$ and $b = \|\widehat{\mathbf{v}}^{n+1}\|_{L^2(\Omega_n^F)}$), we obtain:

$$\rho^F \int_{\Omega_n^F} \frac{\mathbf{v}^n}{\Delta t} \cdot (2\Delta t \widehat{\mathbf{v}}^{n+1}) \leq \rho^F \|\mathbf{v}^n\|^2_{L^2(\Omega_n^F)} + \rho^F \|\widehat{\mathbf{v}}^{n+1}\|^2_{L^2(\Omega_n^F)}.$$

■

**Lemma 8** *The inequality below holds*

$$\int_{\Omega^S} \bar{\mathbf{g}}^{n+1} \cdot (\mathbf{u}^{n+1} - \mathbf{u}^{n-1}) \leq \frac{\Delta t}{\rho^S} \|\bar{\mathbf{g}}^{n+1}\|^2_{L^2(\Omega^S)} + \frac{\rho^S \Delta t}{2} \left\| \frac{\mathbf{u}^{n+1} - \mathbf{u}^n}{\Delta t} \right\|^2_{L^2(\Omega^S)}$$
$$+ \frac{\rho^S \Delta t}{2} \left\| \frac{\mathbf{u}^n - \mathbf{u}^{n-1}}{\Delta t} \right\|^2_{L^2(\Omega^S)}.$$

**Proof.** Multiplying and dividing the term $\int_{\Omega^S} \bar{\mathbf{g}}^{n+1} \cdot (\mathbf{u}^{n+1} - \mathbf{u}^{n-1})$ by $\Delta t$, using Cauchy-Schwarz' inequality and triangular inequality, we obtain

$$\Delta t \int_{\Omega^S} \bar{\mathbf{g}}^{n+1} \cdot \frac{(\mathbf{u}^{n+1} - \mathbf{u}^{n-1})}{\Delta t} \leq \Delta t \sqrt{\frac{2}{\rho^S}} \|\bar{\mathbf{g}}^{n+1}\|_{L^2(\Omega^S)} \sqrt{\frac{\rho^S}{2}} \left\| \frac{\mathbf{u}^{n+1} - \mathbf{u}^{n-1}}{\Delta t} \right\|_{L^2(\Omega^S)}$$
$$\leq \Delta t \sqrt{\frac{2}{\rho^S}} \|\bar{\mathbf{g}}^{n+1}\|_{L^2(\Omega^S)} \sqrt{\frac{\rho^S}{2}} \left( \left\| \frac{\mathbf{u}^{n+1} - \mathbf{u}^n}{\Delta t} \right\|_{L^2(\Omega^S)} + \left\| \frac{\mathbf{u}^n - \mathbf{u}^{n-1}}{\Delta t} \right\|_{L^2(\Omega^S)} \right).$$

From (22), we infer that

$$\int_{\Omega^S} \bar{\mathbf{g}}^{n+1} \cdot (\mathbf{u}^{n+1} - \mathbf{u}^{n-1}) \leq \frac{\rho^S \Delta t}{4} \left( \left\| \frac{\mathbf{u}^{n+1} - \mathbf{u}^n}{\Delta t} \right\|_{L^2(\Omega^S)} + \left\| \frac{\mathbf{u}^n - \mathbf{u}^{n-1}}{\Delta t} \right\|_{L^2(\Omega^S)} \right)^2$$
$$+ \frac{\Delta t}{\rho^S} \|\bar{\mathbf{g}}^{n+1}\|^2_{L^2(\Omega^S)}.$$

Using the inequality $(\alpha + \beta)^2 \leq 2(\alpha^2 + \beta^2)$, we finally have:

$$\int_{\Omega^S} \bar{\mathbf{g}}^{n+1} \cdot (\mathbf{u}^{n+1} - \mathbf{u}^{n-1}) \leq \frac{\rho^S \Delta t}{2} \left\| \frac{\mathbf{u}^{n+1} - \mathbf{u}^n}{\Delta t} \right\|^2_{L^2(\Omega^S)}$$
$$+ \frac{\rho^S \Delta t}{2} \left\| \frac{\mathbf{u}^n - \mathbf{u}^{n-1}}{\Delta t} \right\|^2_{L^2(\Omega^S)} + \frac{\Delta t}{\rho^S} \|\bar{\mathbf{g}}^{n+1}\|^2_{L^2(\Omega^S)}.$$

■

We are going to apply the following lemma (see [24]).

**Lemma 9 (Discrete Gronwall lemma)** *Assume that* $(k_n)_{n \in \mathbb{N}}$ *is a non-ne-*

*gative sequence and that the sequence $\phi_n$ satisfies :*

$$\phi_0 \leq g_0 \;\; et \;\; \phi_n \leq g_0 + \sum_{s=0}^{n-1} p_s + \sum_{s=0}^{n-1} k_s \phi_s, \;\; \forall\, n \geq 1. \tag{23}$$

*Then $\phi_n$ satisfies*

$$\phi_0 \leq g_0(1+k_0)+p_0 \;\; et \;\; \phi_n \leq g_0 \prod_{s=0}^{n-1}(1+k_s)+\sum_{s=0}^{n-2} p_s \prod_{r=s+1}^{n-1}(1+k_r)+p_{n-1}, \;\forall\, n \geq 2. \tag{24}$$

*Moreover, if $g_0 \geq 0$ and $p_n \geq 0$ for $n \geq 0$, it follows*

$$\phi_n \leq \Big(g_0 + \sum_{s=0}^{n-1} p_s\Big) \exp\Big(\sum_{s=0}^{n-1} k_s\Big), \;\; n \geq 1. \tag{25}$$

**Proof.** (Theorem 1) : From (20), using the estimations obtained in the above lemmas, we have:

$$\begin{aligned}
&\rho^F \|\mathbf{v}^{n+1}\|^2_{L^2(\Omega^F_{n+1})} - \rho^F \|\mathbf{v}^n\|^2_{L^2(\Omega^F_n)} + 2\mu^F \Delta t \|\epsilon_{\widehat{\mathbf{x}}}(\widehat{\mathbf{v}}^{n+1})\|^2_{L^2(\Omega^F_n)} \\
&+\rho^S \Big\| \frac{\mathbf{u}^{n+1}-\mathbf{u}^n}{\Delta t} \Big\|^2_{L^2(\Omega^S)} - \rho^S \Big\| \frac{\mathbf{u}^{n}-\mathbf{u}^{n-1}}{\Delta t} \Big\|^2_{L^2(\Omega^S)} + X^{n+1} - X^n \\
&\leq C_2 \Delta t \|\widehat{\mathbf{f}}^{n+1}\|^2_{L^2(\Omega^F_n)} + \frac{\Delta t}{\rho^S} \|\overline{\mathbf{g}}^{n+1}\|^2_{L^2(\Omega^S)} \\
&+\Delta t C' \Big( \|\mathbf{h}^{n+1}_{in}\|^2_{L^2(\Sigma_1)} + \|\mathbf{h}^{n+1}_{out}\|^2_{L^2(\Sigma_3)} \Big) + 2\mu^F \Delta t \|\epsilon_{\widehat{\mathbf{x}}}(\widehat{\mathbf{v}}^{n})\|^2_{L^2(\Omega^F_{n-1})} \\
&+\frac{\rho^S \Delta t}{2} \Big\| \frac{\mathbf{u}^{n+1}-\mathbf{u}^n}{\Delta t} \Big\|^2_{L^2(\Omega^S)} + \frac{\rho^S \Delta t}{2} \Big\| \frac{\mathbf{u}^{n}-\mathbf{u}^{n-1}}{\Delta t} \Big\|^2_{L^2(\Omega^S)}.
\end{aligned}$$

Writing this inequality for all $k = 1, \ldots, n$ and taking the sum over $k$, we get

$$\rho^F\|\mathbf{v}^{n+1}\|^2_{L^2(\Omega^F_{n+1})}+2\mu^F\Delta t\|\epsilon_{\widehat{\mathbf{x}}}(\widehat{\mathbf{v}}^{n+1})\|^2_{L^2(\Omega^F_n)}+\rho^S\left\|\frac{\mathbf{u}^{n+1}-\mathbf{u}^n}{\Delta t}\right\|^2_{L^2(\Omega^S)}$$
$$+X^{n+1}\leq\rho^F\|\mathbf{v}^1\|^2_{L^2(\Omega^F_1)}+2\mu^F\Delta t\|\epsilon_{\widehat{\mathbf{x}}}(\mathbf{v}^1)\|^2_{L^2(\Omega^F_0)}+\rho^S\left\|\frac{\mathbf{u}^1-\mathbf{u}^0}{\Delta t}\right\|^2_{L^2(\Omega^S)}$$
$$+X^1+C_2\Delta t\sum_{k=1}^n\|\widehat{\mathbf{f}}^{k+1}\|^2_{L^2(\Omega^F_k)}+\sum_{k=1}^n\frac{\Delta t}{\rho^S}\|\bar{\mathbf{g}}^{k+1}\|^2_{L^2(\Omega^S)}$$
$$+\Delta tC'\Big(\sum_{k=1}^n\|\mathbf{h}^{k+1}_{in}\|^2_{L^2(\Sigma_1)}+\sum_{k=1}^n\|\mathbf{h}^{k+1}_{out}\|^2_{L^2(\Sigma_3)}\Big)+\frac{\rho^S\Delta t}{2}\left\|\frac{\mathbf{u}^1-\mathbf{u}^0}{\Delta t}\right\|^2_{L^2(\Omega^S)}$$
$$+\sum_{k=1}^{n-1}\rho^S\Delta t\left\|\frac{\mathbf{u}^{k+1}-\mathbf{u}^k}{\Delta t}\right\|^2_{L^2(\Omega^S)}+\frac{\rho^S\Delta t}{2}\left\|\frac{\mathbf{u}^{n+1}-\mathbf{u}^n}{\Delta t}\right\|^2_{L^2(\Omega^S)}. \tag{26}$$

On the other hand, we have:

$$C_2\Delta t\sum_{k=1}^n\|\widehat{\mathbf{f}}^{k+1}\|^2_{L^2(\Omega^F_k)}+\sum_{k=1}^n\frac{\Delta t}{\rho^S}\|\bar{\mathbf{g}}^{k+1}\|^2_{L^2(\Omega^S)}$$
$$+\Delta tC'\Big(\sum_{k=1}^n\|\widehat{\mathbf{h}}^{k+1}_{in}\|^2_{L^2(\Sigma_1)}+\sum_{k=1}^n\|\widehat{\mathbf{h}}^{k+1}_{out}\|^2_{L^2(\Sigma_3)}\Big)$$
$$\leq\Delta t\Big(nC_2\max_{t\in[0,T]}\|\mathbf{f}^F(t)\|^2_{L^2(\Omega^F_t)}+\frac{n}{\rho^S}\max_{t\in[0,T]}\|\mathbf{f}^S(t)\|^2_{L^2(\Omega^S)}$$
$$+nC'\max_{t\in[0,T]}\|\mathbf{h}_{in}(t)\|^2_{L^2(\Sigma_1)}+nC'\max_{t\in[0,T]}\|\mathbf{h}_{out}(t)\|^2_{L^2(\Sigma_3)}\Big)$$

and by using that $n\Delta t<T$, we get

$$C_2\Delta t\sum_{k=1}^n\|\widehat{\mathbf{f}}^{k+1}\|^2_{L^2(\Omega^F_k)}+\sum_{k=1}^n\frac{\Delta t}{\rho^S}\|\bar{\mathbf{g}}^{k+1}\|^2_{L^2(\Omega^S)}$$
$$+\Delta tC'\Big(\sum_{k=1}^n\|\mathbf{h}^{k+1}_{in}\|^2_{L^2(\Sigma_1)}+\sum_{k=1}^n\|\mathbf{h}^{k+1}_{out}\|^2_{L^2(\Sigma_3)}\Big)$$
$$\leq T\Big(C_2\max_{t\in[0,T]}\|\mathbf{f}^F(t)\|^2_{L^2(\Omega^F_t)}+\frac{1}{\rho^S}\max_{t\in[0,T]}\|\mathbf{f}^S(t)\|^2_{L^2(\Omega^S)}$$
$$+C'\max_{t\in[0,T]}\|\mathbf{h}_{in}(t)\|^2_{L^2(\Sigma_1)}+C'\max_{t\in[0,T]}\|\mathbf{h}_{out}(t)\|^2_{L^2(\Sigma_3)}\Big).$$

In this way, we have obtained an upper bound of the terms depending on $\mathbf{f}^F$, $\mathbf{f}^S$, $\mathbf{h}_{in}$, $\mathbf{h}_{out}$ which appear in the right-hand side of (26).

Let us set

$$\phi_n = \rho^F \|\mathbf{v}^{n+1}\|^2_{L^2(\Omega^F_{n+1})} + 2\mu^F \Delta t \|\epsilon_{\widehat{\mathbf{x}}}(\widehat{\mathbf{v}}^{n+1})\|^2_{L^2(\Omega^F_n)}$$
$$+\rho^S \left\| \frac{\mathbf{u}^{n+1} - \mathbf{u}^n}{\Delta t} \right\|^2_{L^2(\Omega^S)} + X^{n+1},$$

we get that the sum of the last three terms in (26) is dominated by:

$$\frac{\rho^S \Delta t}{2} \left\| \frac{\mathbf{u}^1 - \mathbf{u}^0}{\Delta t} \right\|^2_{L^2(\Omega^S)} + \sum_{k=1}^{n-1} \rho^S \Delta t \left\| \frac{\mathbf{u}^{k+1} - \mathbf{u}^k}{\Delta t} \right\|^2_{L^2(\Omega^S)}$$
$$+\frac{\rho^S \Delta t}{2} \left\| \frac{\mathbf{u}^{n+1} - \mathbf{u}^n}{\Delta t} \right\|^2_{L^2(\Omega^S)} \leq \sum_{k=0}^{n} \rho^S \Delta t \left\| \frac{\mathbf{u}^{k+1} - \mathbf{u}^k}{\Delta t} \right\|^2_{L^2(\Omega^S)}$$
$$\leq \Delta t(\phi_0 + \cdots + \phi_n).$$

We set also:

$$g_0 = \rho^F \|\mathbf{v}^1\|^2_{L^2(\Omega^F_1)} + 2\mu^F \Delta t \|\epsilon_{\widehat{\mathbf{x}}}(\widehat{\mathbf{v}}^1)\|^2_{L^2(\Omega^F_0)} + \frac{\rho^S}{2} \left\| \frac{\mathbf{u}^1 - \mathbf{u}^0}{\Delta t} \right\|^2_{L^2(\Omega^S)} + X^1$$
$$+T\Big( C_2 \max_{t\in[0,T]} \|\mathbf{f}^F\|^2_{L^2(\Omega^F_t)} + \frac{1}{\rho^S} \max_{t\in[0,T]} \|\mathbf{f}^S\|^2_{L^2(\Omega^S)}$$
$$+C' \max_{t\in[0,T]} \|\mathbf{h}_{in}\|^2_{L^2(\Sigma_1)} + C' \max_{t\in[0,T]} \|\mathbf{h}_{out}\|^2_{L^2(\Sigma_3)} \Big),$$

then $\phi_0 \leq g_0$ and let us take $p_s = 0$, $k_s = \Delta t$. So the Gronwall lemma assumptions are satisfied, thus we may apply it now with sum from 0 to $n$, we get:

$$\rho^F \|\mathbf{v}^{n+1}\|^2_{L^2(\Omega^F_{n+1})} + 2\mu^F \Delta t \|\epsilon_{\widehat{\mathbf{x}}}(\widehat{\mathbf{v}}^{n+1})\|^2_{L^2(\Omega^F_n)} + \rho^S \left\| \frac{\mathbf{u}^{n+1} - \mathbf{u}^n}{\Delta t} \right\|^2_{L^2(\Omega^S)}$$
$$+X^{n+1} \leq \left[ \rho^F \|\mathbf{v}^1\|^2_{L^2(\Omega^F_1)} + 2\mu^F \Delta t \|\epsilon(\widehat{\mathbf{v}}^1)\|^2_{L^2(\Omega^F_0)} + \rho^S \left\| \frac{\mathbf{u}^1 - \mathbf{u}^0}{\Delta t} \right\|^2_{L^2(\Omega^S)} \right.$$
$$+X^1 + T\Big( C_2 \max_{t\in[0,T]} \|\mathbf{f}^F(t)\|^2_{L^2(\Omega^F_t)} + \frac{1}{\rho^S} \max_{t\in[0,T]} \|\mathbf{f}^S(t)\|^2_{L^2(\Omega^S)}$$
$$\left. +C' \max_{t\in[0,T]} \|\mathbf{h}_{in}(t)\|^2_{L^2(\Sigma_1)} + C' \max_{t\in[0,T]} \|\mathbf{h}_{out}(t)\|^2_{L^2(\Sigma_3)} \Big) \right] \exp(T), \tag{27}$$

since $\sum_{s=0}^{n} k_s = (n+1)\Delta t \leq T$.

We obtain the expected inequality by setting $C = T \max(C_2, C', \frac{1}{\rho^S})$. Further-

more, we can remark that

$$X^{n+1} = \Big(\frac{4\theta-1}{2}\Big)\Big[a_s(\mathbf{u}^{n+1},\mathbf{u}^{n+1}) + a_S(\mathbf{u}^n,\mathbf{u}^n)\Big]$$
$$+\Big(\frac{1-2\theta}{2}\Big)a_S(\mathbf{u}^{n+1}+\mathbf{u}^n,\mathbf{u}^{n+1}+\mathbf{u}^n),$$

If $\theta \in \Big[\frac{1}{4},\frac{1}{2}\Big]$, then $X^n \geq 0$ for any $n$. Which implies from (27) that

$$\rho^F\|\mathbf{v}^{n+1}\|^2_{L^2(\Omega^F_{n+1})},\ 2\mu^F\Delta t\|\epsilon(\widehat{\mathbf{v}}^{n+1}),\ \|^2_{L^2(\Omega^F_n)},\ \frac{\rho^S}{2}\Big\|\frac{\mathbf{u}^{n+1}-\mathbf{u}^n}{\Delta t}\Big\|^2_{L^2(\Omega^S)},\ \text{and } X^{n+1}$$

are bounded. ■

## 6 Algorithm implementation

The monolithic linear system (20) can be solved by finite element method and the continuity of the velocity at the interface must be satisfied as an essential boundary condition. The fluid test functions must coincide with the structure test functions at the interface, implying some constraints for triangulation of the fluid and structure domains as well as in the choice of the finite elements. In [20], a related problem has been solved, using the Augmented Lagrangian Method where the continuity of the velocity was treated by a Lagrange multiplier. The numerical results presented in [20] show that the continuity of the velocity is not very well respected since the error in the $L^2$ norm between the fluid and structure velocity at the interface is 0.45.

The method that we use here to solve the coupled problem is based on partitioned procedure (the fluid and structure equations are solved separately), which is very often used to solve fluid-structure interaction problem. At each

time step, an optimization problem in the form

$$\inf_{\alpha \in \mathbb{R}^m} J(\alpha)$$

has to be solved, where $\sum_{i=1}^{m} \alpha_i \phi_i$ is an approximation of the stress at the fluid-structure interface. The shape functions $\phi_i$, $i = 1, \ldots, m$ defined at the interface are orthonormal with respect to the scalar product in $L^2$. This technique was successfully employed in [19], [17], where implicit algorithms are presented. We will use the same least square method based on the Broyden, Fletcher, Goldford, Shano (BFGS) method in order to identify the stress at the interface.

We present below the implicit algorithm. More details can be found in [19].

**Implicit algorithm**

**Step 1** Solve by BFGS the optimization problem

$$\alpha^{n+1} \in \arg\min_{\alpha \in \mathbb{R}^m} J(\alpha),$$

where the cost function is computed as follows:

- Let $\sum_{i=1}^{m} \alpha_i \phi_i$ be a guess of the stress at the fluid-structure interface.
- Solve the structure problem under the load $\sum_{i=1}^{m} \alpha_i \phi_i$ at the interface to get the displacement $\mathbf{u}$.
- Build a fluid mesh $\mathcal{T}$ depending on the displacement $\mathbf{u}$.
- Solve the fluid problem on the mesh $\mathcal{T}$ under prescribed velocity at the fluid-structure interface in order to get the fluid velocity $\mathbf{v}$ and pressure $p$.
- Compute $\beta_i = -\int_{\Gamma_0} \left( \sigma^F (\mathbf{v}, p)\, \mathbf{n}^F \right) \cdot \phi_i(X)\, \omega(X, t)$ for $i = 1, \ldots, m$.
- Set the cost function

$$J(\alpha) = \frac{1}{2} \|\alpha - \beta\|^2_{\mathbb{R}^m}$$

**Step 2** Save the mesh $\mathcal{T}^{n+1}$, the structure displacement $\mathbf{u}^{n+1}$, the fluid velocity $\mathbf{v}^{n+1}$, the fluid pressure $p^{n+1}$ obtained at the last iteration of the BFGS algorithm at **Step 1**.

**Remark 5** *We emphasize that in the implicit strategy, the fluid mesh changes at each call of the cost function during the minimization process.*

**Semi-implicit algorithm**

**Step 1** Compute the mesh velocity $\boldsymbol{\vartheta}^n$ from (18).

**Step 2** Assembling the finite element matrix of fluid problem (14) using the mesh $\mathcal{T}^n$ obtained at the previous time step. Get a LU factorization of the matrix.

**Step 3** Solve by BFGS the optimization problem using the fluid frozen mesh $\mathcal{T}^n$

$$\alpha^{n+1} \in \arg\min_{\alpha \in \mathbb{R}^m} J(\alpha),$$

where the cost function is computed as follows:

- Let $\sum_{i=1}^m \alpha_i \phi_i$ be a guess of the stress at the fluid-structure interface.
- Solve the structure problem under the load $\sum_{i=1}^m \alpha_i \phi_i$ at the interface to get the displacement $\mathbf{u}$.
- Solve the fluid problem on the mesh $\mathcal{T}^n$ under prescribed velocity at the fluid-structure interface in order to get the fluid velocity $\mathbf{v}$ and pressure $p$.
- Compute $\beta_i = -\int_{\Gamma_0} \left(\sigma^F(\mathbf{v}, p)\,\mathbf{n}^F\right) \cdot \phi_i(X)\,\omega(X,t)$ for $i = 1, \ldots, m$.
- Set the cost function

$$J(\alpha) = \frac{1}{2}\|\alpha - \beta\|^2_{\mathbb{R}^m}$$

**Step 4** Build mesh $\mathcal{T}^{n+1}$, as the image of $\mathcal{T}^n$ by the map $\widehat{x} \mapsto \widehat{x} + \Delta t \boldsymbol{\vartheta}^n(\widehat{x})$

and save the mesh $\mathcal{T}^{n+1}$, the fluid velocity $\mathbf{v}^{n+1}(\mathbf{x}) = \widehat{\mathbf{v}}^{n+1}(\widehat{\mathbf{x}})$, etc.

**Remark 6** *Contrary to the implicit strategy, the semi-implicit one use a fixed fluid mesh during the iterative method for solving the optimization problem, which reduces considerably the computational time.*

The BFGS is a gradient like algorithm for solving unconstrained optimization problems. We approximate the gradient of the cost function by a first order finite difference scheme which requires $m + 1$ evaluations of the cost function. We recall that $m$ is the number of the shape functions used to compute the stress at the fluid-structure interface. Therefore, it is important to work with small values of $m$. The shape functions $\phi_i$ are not necessary compatible with the structure or fluid finite element functions. Possible choices for $\phi_i$ are polynomial functions [18], finite element like functions, eigenfunctions associated to the structure equations [19], [17]. In the case where the $\phi_i$ are not orthonormal for the scalar product of $L^2$ at the interface, the cost function has the form

$$J(\alpha) = \frac{1}{2} \int_{\Gamma_0} \left( \sum_{i=1}^{m} \alpha_i \phi_i(X) - \sigma^F(\mathbf{v}, p)\, \mathbf{n}^F\, \omega(X,t) \right)^2 dX.$$

In this paper, we have chosen $\phi_i$ as the eigenfunctions associated to the structure equations. Since the eigenfunctions are orthonormal, the cost function has the form

$$J(\alpha) = \frac{1}{2} \|\alpha - \beta\|^2_{\mathbb{R}^m}$$

where $\beta_i = -\int_{\Gamma_0} \left( \sigma^F(\mathbf{v}, p)\, \mathbf{n}^F \right) \cdot \phi_i(X)\, \omega(X,t)\, dX$.

In this paper, for convenience, the structure problem (15) is solved numerically by modal decomposition. We set $\mathbf{u}(X,t) = \sum_{i \geq 1} q_i(t) \phi_i(X)$. The structure

problem is: find $q_i^{n+1}$ such that

$$\frac{q_i^{n+1}-2q_i^n+q_i^{n-1}}{(\Delta t)^2}+\lambda_i(\theta q_i^{n+1}+(1-2\theta)q_i^n+\theta q_i^{n-1})=\theta\alpha_i^{n+1}+(1-2\theta)\alpha_i^n+\theta\alpha_i^{n-1},$$

where $\lambda_i$ is the eigenvalue associated to the eigenfunction $\phi_i$ and $\alpha_i^{n+1} = \alpha_i(t_{n+1}) = \int_{\Gamma_0}(\sigma^S\mathbf{n}^S)\phi_i(X)\,dX$. We have assumed that $\mathbf{f}^S = (0,\,0)$. The modal decomposition is efficient only in the context of linear model for the structure. For a non-linear model, the structure problem could be solved by an appropriate finite element method, independent of choice of the shape functions used to approach the stress at the fluid-structure interface. We will study this aspect in a future work.

## 7 Numerical results

### *7.1 Flow in a flexible straight tube*

*Physical parameters*

We consider the following data for the computation: the length of the fluid domain is L= 6 $cm$ and its height is $H = 1$ $cm$. The viscosity of the fluid was fixed to be $\mu = 0.035\ \frac{g}{cm\cdot s}$, its density $\rho^F = 1\ \frac{g}{cm^3}$ and the volume force in fluid is $\mathbf{f}^F = (0,\,0)^T$. The prescribed boundary stress at the outflow is $\mathbf{h}_{out}(x,t) = (0,\,0)$ and at the inflow is

$$\mathbf{h}_{in}(x,t) = \begin{cases} (10^3(1-\cos(2\pi t/0.025)),\,0),\ x\in\Sigma_1, 0\le t\le 0.025 \\ (0,\,0), \qquad\qquad\qquad\qquad x\in\Sigma_1, 0.025\le t\le T. \end{cases}$$

The thickness of the elastic wall is $h^S = 0.1$ $cm$, the Young modulus $E =$

$3 \cdot 10^6$ $\frac{g}{cm \cdot s^2}$, the Poisson ratio $\nu = 0.3$, the mass density $\rho^S = 1.1 \frac{g}{cm^3}$ and the volume force is $\mathbf{f}^S = (0,\, 0)^T$. The Lamé's coefficients are computed by the formulas:

$$\lambda^S = \frac{\nu^S E}{(1 - 2\nu^S)}(1 + \nu^S), \qquad \mu^S = \frac{E}{2(1 + \nu^S)}.$$

The structure is supposed to be fixed at the left and at the right sides.

*Numerical parameters*

The numerical tests have been performed using FreeFem++ (see [15]). We have used for the structure a reference mesh of 60 triangles and 62 vertices and for the fluid a reference mesh of 1250 triangles and 696 vertices. The meshes are not necessary compatible at the interface (see Figure 4). For the approximation of the fluid velocity and pressure, we have employed the triangular finite element $\mathbb{P}_1 + bubble$ and $\mathbb{P}_1$ respectively. The finite element $\mathbb{P}_1$ was used in order to solve the eigenproblem of the structure. Only the first $m = 3$ modes have been considered. The first eigenvalues are $\lambda_{1,h} = 7018.91$, $\lambda_{2,h} = 50500$ and $\lambda_{3,h} = 193418$. The real parameter in the $\theta$-centered scheme was chosen to be $\theta = 0.3$.

*Stopping criteria*

At each time step, the optimization problem have been solved by the BFGS algorithm. We have used the FreeFem++ implementation of the BFGS algorithm which use the stopping criteria: $\|\nabla J\| \leq \epsilon$ or the number of iterations reaches a maximal value *nbiter*. We have performed the computation with $\epsilon = 10^{-4}$ and $nbiter = 10$. We set to 5 maximal number of the iterations for the time search. The final values of the cost function are less than $6.10^{-12}$. In other words, the continuity of the velocity at the interface holds at every time

step, while the error between the fluid and structure stress at the interface is less than $6.10^{-12}$. This implies that $\|\Delta q_i^{n+1}\|$ is less than $10^{-13}$.

*Behavior of the computed solution*

We have performed the simulation for a time duration $T = 0.1\ s$, with time step $\Delta t = 0.001$ and number of iterations in time $N = 100$. We have compared the vertical displacements of three points at the interface between the semi-implicit and the implicit algorithm. Figure 2 shows that the solution computed by the semi-implicit algorithm is similar to the one obtained by the implicit algorithm.

We have proved that the time stability of the algorithm does not depend on the time step. The vertical displacements of three points at the interface for time steps $\Delta t = 0.001\ s$, $\Delta t = 0.0005\ s$ and $\Delta t = 0.0025\ s$ are presented in Figure 3. We observe that the vertical displacements are less than 0.3 cm. For $\Delta t = 0.001\ s$, the fluid pressure and velocity at different time instants are plotted in Figures 5 and 6.

*CPU time*

Here, we will compare the CPU time obtained using the semi-implicit time strategy algorithm proposed in this paper with the CPU time obtained by the implicit time advancing algorithm. The computation has been made on a computer with one processor of 1.66 GHz frequency and 2 Gb RAM. To compare the computational time between implicit and semi-implicit strategies is mandatory to use the same algorithm for solving the fluid-structure coupled problem at every time step. We emphasize that in the case of implicit

strategy the coupled fluid-structure problem is non-linear due to the moving domain, contrary to the semi-implicit strategy, where the coupled problem (20) is linear.

We denote by $m$ the number of eigenfunctions in the modal decomposition of the structure problem and $h$ the mesh seize, $nv$ the number of vertices, $nt$ the number of triangles of the fluid domain.

(1) The CPU time in function of $m$, when the time step is $\Delta t = 0.001s$, the number of steps is $N = 100$, the mesh parameters of fluid are $nv = 696$ and $nt = 1250$ triangles:

| m | CPU-semi-implicit | CPU-implicit | $\frac{CPU-implicit}{CPU-semi}$ |
|---|---|---|---|
| 3 | 8 m 30 s | 92 m 30 s | 11.12 |
| 7 | 21 m 44 s | 227 m 53 s | 10.62 |
| 10 | 29 m 54 s | 304 m 22 s | 10.30 |

(2) The CPU time in function of fluid mesh size, when $\Delta t = 0.001$, $N = 100$ and $m = 3$:

| $nv$ | $nt$ | $h$ | CPU-semi-implicit | CPU-implicit | $\frac{CPU-implicit}{CPU-semi}$ |
|---|---|---|---|---|---|
| 696 | 1250 | 0.16 | 8 m 30 s | 92 m 30 s | 11.12 |
| 1632 | 3052 | 0.11 | 19m 48 s | 226 m 42 s | 11.62 |
| 2664 | 5046 | 0.08 | 33 m 50 s | 415 m 23 s | 12.39 |

(3) The CPU time in function of $\Delta t$, when $m = 3$, $nv = 696$ and $nt = 1250$:

| $\Delta t$ | N | CPU-semi-implicit | CPU-implicit | $\frac{CPU-implicit}{CPU-semi}$ |
|---|---|---|---|---|
| 0.0005 | 200 | 14 m 48 s | 187 m 47 s | 12.95 |
| 0.0010 | 100 | 8 m 30 s | 92 m 30 s | 11.12 |
| 0.0025 | 40 | 3 m 27 s | 36 m 24 s | 11.08 |

*The mean number of cost function calls by time step*

At each time step, the BFGS performs on average 5.47 iterations in the semi-implicit case and 6.93 iterations in the implicit case. At each BFGS iteration, 2.68 evaluations of the cost function are necessary on average for the line search in the semi-implicit case and 2.60 iterations in the implicit case. One call of the gradient is necessary at each BFGS iteration for the both semi-implicit and implicit strategies. We compute the gradient $\nabla J(\alpha)$ by finite difference scheme:

$$\frac{\partial J}{\partial \alpha_k}(\alpha) = \frac{J(\alpha + \Delta\alpha_k e_k) - J(\alpha)}{\Delta\alpha_k}$$

where $e_k$ is the $k$-th vector of the canonical base of $\mathbb{R}^m$ and $\Delta\alpha_k = 10^{-6}$ is the grid spacing. Thus, $m + 1 = 4$ calls of the cost function are needed to compute the gradient. To sum up, at each time step, the BFGS performs in average 36.59 evaluations of the cost function in the semi-implicit case and 45.80 iterations in the implicit case. We recall that, contrary to the implicit strategy, the semi-implicit one uses a fixed fluid mesh for all calls of the cost function at a time instant, which explains the reduction of the computational time.

*Geometry*

The bottom of the fluid domain is $\Sigma_2$ the horizontal $[-1,7]\times\{0\}$. The inflow $\Sigma_1 = \{-1\}\times[0,1]$ and outflow $\Sigma_3 = \{7\}\times[0,1]$ sections are vertical segments of length 1 cm. The top boundary $\Gamma_0$ of the undeformed fluid domain is composed by three curves: at the left

$$\left\{x_1 = \xi,\ x_2 = 0.1\xi^3 + 0.4\xi^2 + 0.5\xi + 1,\ \xi \in [-1,0]\right\}$$

in the middle

$$\left\{(x_1,x_2)\in\mathbb{R}^2;\ x_1 = \xi,\ x_2 = -5 + \sqrt{45-(\xi-3)^2},\ \xi\in[0,L]\right\}$$

where $L = 6$ and at the right

$$\left\{x_1 = \xi,\ x_2 = -0.1\xi^3 + 2.2\xi^2 - 16.1\xi + 40,\ \xi\in[6,7]\right\}.$$

As in the previous test, the top boundary is flexible. The initial geometrical configuration is presented in Figure 7.

*Physical and numerical parameters*

The thickness of the elastic wall is $h^S = 0.1\ cm$ and the left and the right sides are fixed. We have used for the structure a reference mesh of 80 triangles and 82 vertices and for the fluid a reference mesh of 1216 triangles and 672 vertices. The meshes are not necessary compatible at the interface.

We have performed the simulation using the time step $\Delta t = 0.001$ and $N = 120$ time increments. The others physical and numerical parameters are the same as in the previous test.

The fluid velocity computed by the semi-implicit algorithm at different time instants is plotted in Figures 8. The vertical displacement of three points at the interface of horizontal coordinates $x_1 = 1.5$, $x_1 = 3$, $x_1 = 4.5$, respectively, are presented in Figure 9. We recall that the left and right sides of the fluid domain are vertical segments of horizontal coordinates $x_1 = -1$ and $x_1 = 7$, respectively. We observe that the vertical displacements are less than 0.2 cm.

*CPU time for small time step*

In addition, we have performed the simulation for a small time step $\Delta t = 10^{-6}$. In this case, the BFGS algorithm finds the solution after 2.68 iterations in average, while for a medium time step $\Delta t = 10^{-3}$ the mean number of BFGS iterations was 5.47. The above results have been obtained using the semi-implicit strategy. The mean number of cost function calls at a time instant is 17.74 for $\Delta t = 10^{-6}$, while for $\Delta t = 10^{-3}$, the number of cost function calls was 36.59. When the time step is small, the starting point for the optimization problem is close to the solution, which explains the reduction of the cost function calls. The CPU time for $N = 50$ time iterations and $\Delta t = 10^{-6}$ is 152s when the semi-implicit strategy is used and 689s in the implicit case. The reduction factor of CPU time is 4.53.

**Future works**

We intend to apply the semi-implicit algorithm presented in this paper to realistic applications in haemodynamics and actually we are looking for a three-dimensional computational environment. The partitioned procedures technique employed to solve the coupled fluid-structure problem allowss us to

employ existing solvers for each sub-problem. We need a structure solver, a solver for Navier-Stokes equations in moving domains and an optimization module. Let us remark that, once the fluid domain is computed by extrapolation, then the structure and the fluid sub-problems could be solved in parallel. We intent to replace the linear model for the structure by a non-linear one which handles large displacements.

## Conclusions

A semi-implicit time advancing scheme for transient fluid-structure interaction problem was presented. For the fluid equations, we consider an implicit Euler scheme for the time derivative and the convection term was linearized. For the structure, we employ a $\theta$-centered scheme of second-order in time. At every time step, a least squares problem is solved by partitioned procedures, such that the continuity of the velocity as well as the continuity of the stress hold at the interface. During the iterative method for solving the optimization problem, the fluid mesh does not move, which reduces the computational effort. The unconditional stability of the algorithm was proved. The numerical results presented in this paper show that the computed solution is similar to the one obtained by the implicit algorithm, but the computational time is reduced.

## References

[1] K.J. Bathe, H. Zhang, Finite element developments for general fluid flows with structural interactions, Int. J. Numer. Meth. Engng. 60 (2004) 213–232.

[2] L. Baffico, A characteristic-ALE formulation for a fluid-membrane interaction problem, Comm. Numer. Methods Engrg. 21 (2005) 723–734.

[3] Z.X. Cai, X.Y. Luo, A fluid-beam model for flow in collapsible channel, Journal of Fluids and Structures, 17 (2003) 125–146.

[4] P. Causin, J.F. Gerbeau, F. Nobile, Added-mass effect in the design of partitioned algorithms for fluid-structure problems. Comput. Methods Appl. Mech. Engrg. 194 (2005) 4506–4527.

[5] S. Deparis, M. Discacciati, A. Quarteroni, Fluid-structure algorithms based on Steklov-Poincaré operators. Comput. Methods Appl. Mech. Engrg. 195 (2006) 5797–5812.

[6] W. Dettmer, D. Perić, A computational framework for fluid-structure interaction: Finite element formulation and applications. Comput. Methods Appl. Mech. Engrg. 195 (2006) 5754-5779.

[7] G. Duvaut, Mécanique des milieux continus, Masson, Paris, 1990.

[8] C. Farhat, M. Lesoinne, Two efficient staggered algorithms for the serial and parallel solution of three-dimensional nonlinear transient aeroelastic problems, Comput. Methods Appl. Mech. Engrg. 182 (2000) 499–515.

[9] M.A. Fernàndez, M. Moubachir, A Newton method using exact jacobians for solving fluid-structure coupling. Comput. & Structures, 83 (2005) 127-142.

[10] M.A. Fernàndez, J.-F. Gerbeau, C. Grandmont, A projection semi-implicit scheme for the coupling of an elastic structure with an incompressible fluid, Internat. J. Numer. Methods Engrg. 69 (2007) no. 4, 794–821.

[11] L. Formaggia, G.F. Gerbeau, F. Nobile, A. Quarteroni, On the coupling of 3D and 1D Navier-Stokes equations for flow problems in compliant vessels. Comput. Methods Appl. Mech. Engrg. 191 (2001) 561–582.

[12] C. Forster, W.A. Wall, E. Ramm, Artificial added mass instabilities in sequential staggered coupling of nonlinear structures and incompressible viscous flows. Comput. Methods Appl. Mech. Engrg. 196 (2007) 1278–1293.

[13] C. Grandmont, V. Guimet, Y. Maday, Numerical analysis of some decoupling techniques for the approximation of the unsteady fluid structure interaction. Math. Models Methods Appl. Sci. 11 (2001), no. 8, 1349–1377.

[14] G.F. Gerbeau, M. Vidrascu, A quasi-Newton algorithm on a reduced model for fluid-structure interaction problems in blood flows. Math. Model. Num. Anal., 37 (2003) 631-648.

[15] F. Hecht, O. Pironneau, A. Le Hyaric, K. Ohtsuka, FreeFem++: http://www.freefem++.org/ff++.

[16] P. Le Tallec, J. Mouro, Fluid-structure interaction with large structural displacements. Comput. Methods Appl. Mech. Engrg. 190 (2001) 3039–3067.

[17] I. Mbaye, C.M. Murea, Numerical procedure with analytic derivative for unsteady fluid-structure interaction. Commun. Numer. Meth. Engng. Published Online: July 13, 2007, DOI: 10.1002/cnm.1031

[18] C.M. Murea, The BFGS algorithm for a nonlinear least squares problem arising from blood flow in arteries, Comput. Math. Appl., 49 (2005) 171–186.

[19] C.M. Murea, Numerical simulation of a pulsatile flow through a flexible channel. ESAIM: Math. Model. Numer. Anal., 40 (2006) 1101–1125.

[20] C.M. Murea, A semi-implicit algorithm based on the Augmented Lagragian Method for fluid-structure interface. Proceeding of ENUMAT 07 Graz, Steptember 10-17, 2007, submitted.

[21] F. Nobile, Numerical approximation of fluid-structure interaction problems with application to haemodynamics. Ph.D. Thesis, EPFL, Switzerland, 2001.

[22] F. Nobile, C. Vergara, An effective fluid-structure interaction formulation for vascular dynamics by generalized Robin conditions. MOX Report 01/2007.

[23] A. Quarteroni, L. Formaggia, Mathematical modelling and numerical simulation of the cardiovascular system, in P.G. Ciarlet (Ed.), Handbook of numerical analysis, Vol. XII, North-Holland, Amsterdam, 2004, 3–127.

[24] A. Quarteroni, A. Valli, Numerical approximation of PDE, Springer, Berlin, New York, 1997.

[25] J. Steindorf, H.B. Matthies, Partioned but strongly coupled iteration schemes for nonlinear fluid-structure interaction, Comput. & Structures, 80 (2003) 1991–1999.

[26] E.W. Swim, P. Seshaiyer, A nonconforming finite element method for fluid-structure interaction problems, Comput. Methods Appl. Mech. Engrg. 195 (2006) 2088–2099.

[27] T.E. Tezduyar, S. Sathe, R. Keedy, K. Stein, Space-time finite element techniques for computation of fluid-structure interactions, Comp. Meth. Appl. Mech. Engng., 195 (2006) 2002–2027.

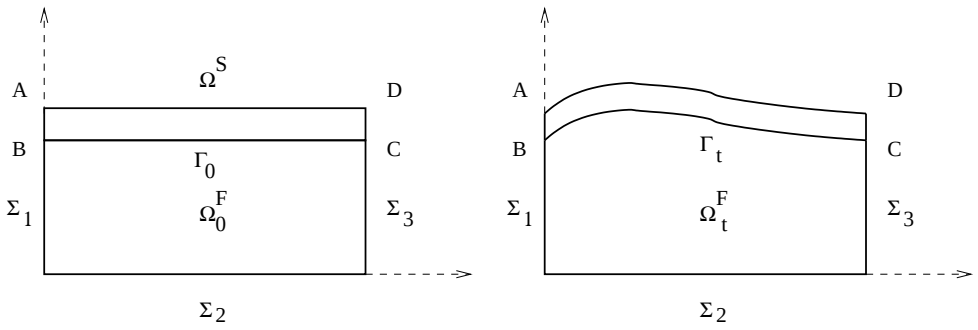


Fig. 1. Initial configuration (left) and intermediate configuration (right).

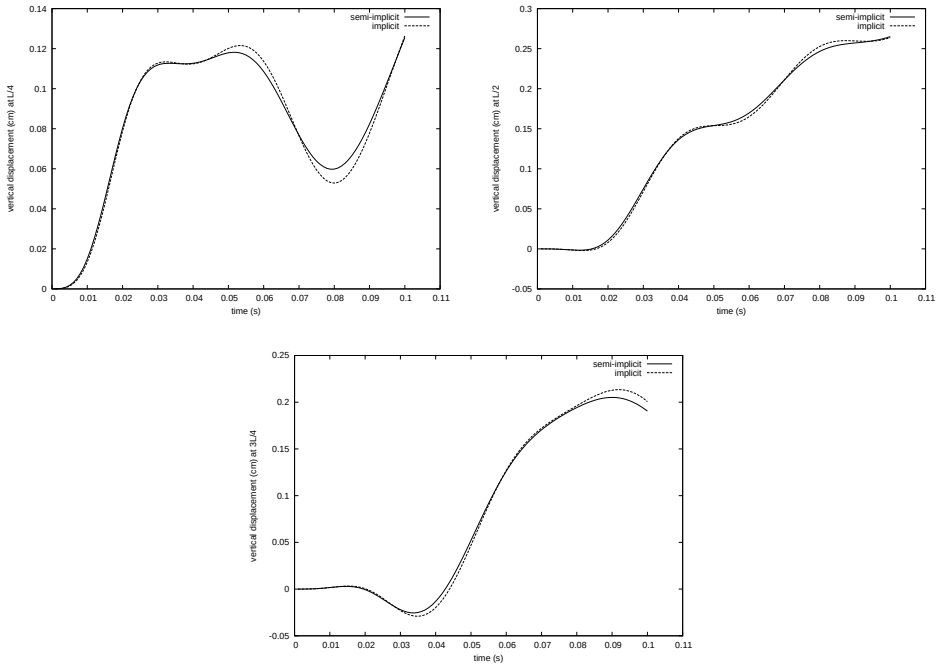


Fig. 2. Vertical displacement when $\Delta t = 0.001s$ of three points at the interface of horizontal coordinates $x_1 = \frac{L}{4}$, (top, left) $x_1 = \frac{L}{2}$, (top, right), $x_1 = \frac{3L}{4}$ (bottom) for the semi-implcit case and the implicit case.

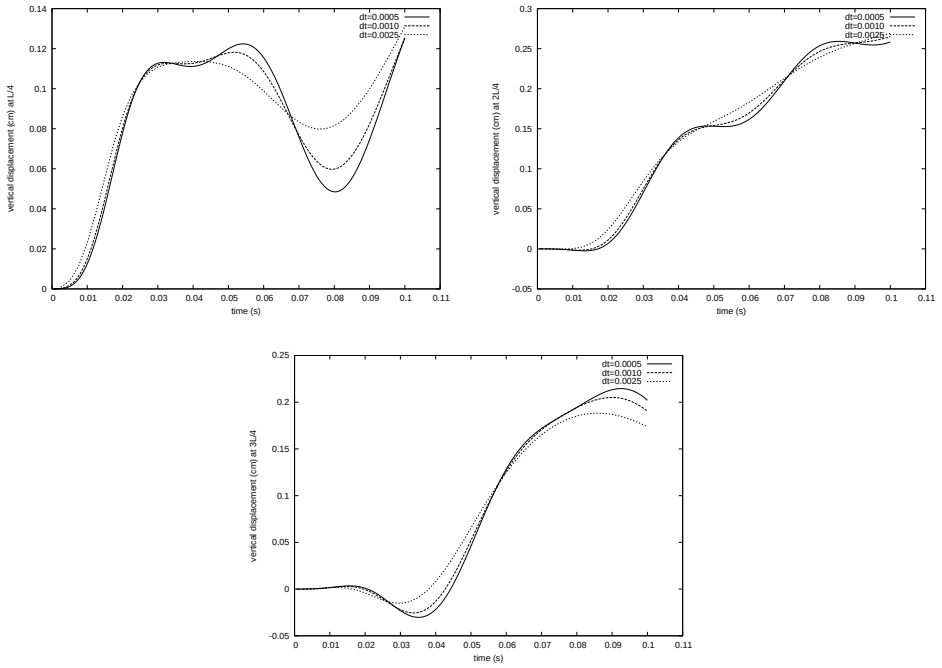


Fig. 3. Vertical displacement when $\Delta t = 0.001s$, $\Delta t = 0.0005s$, $\Delta t = 0.0025s$ of three points at the interface of horizontal coordinates $x_1 = \frac{L}{4}$ (top, left), $x_1 = \frac{L}{2}$ (top, right), $x_1 = \frac{3L}{4}$ (bottom).

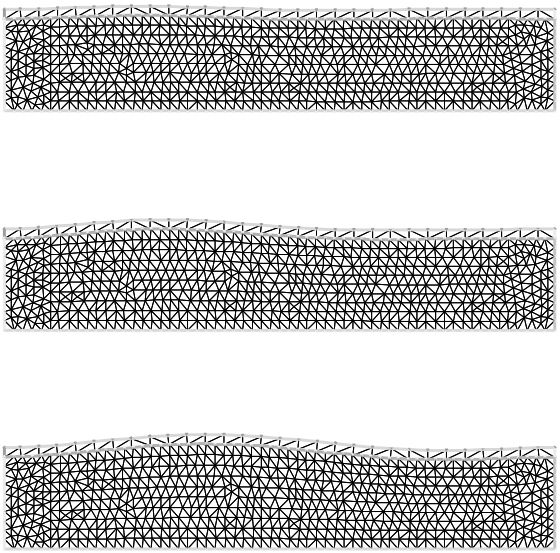

Fig. 4. Fluid and structure meshes at time instant $t = 0.015$ (top), $t = 0.025$ (middle), $t = 0.035$ (bottom)

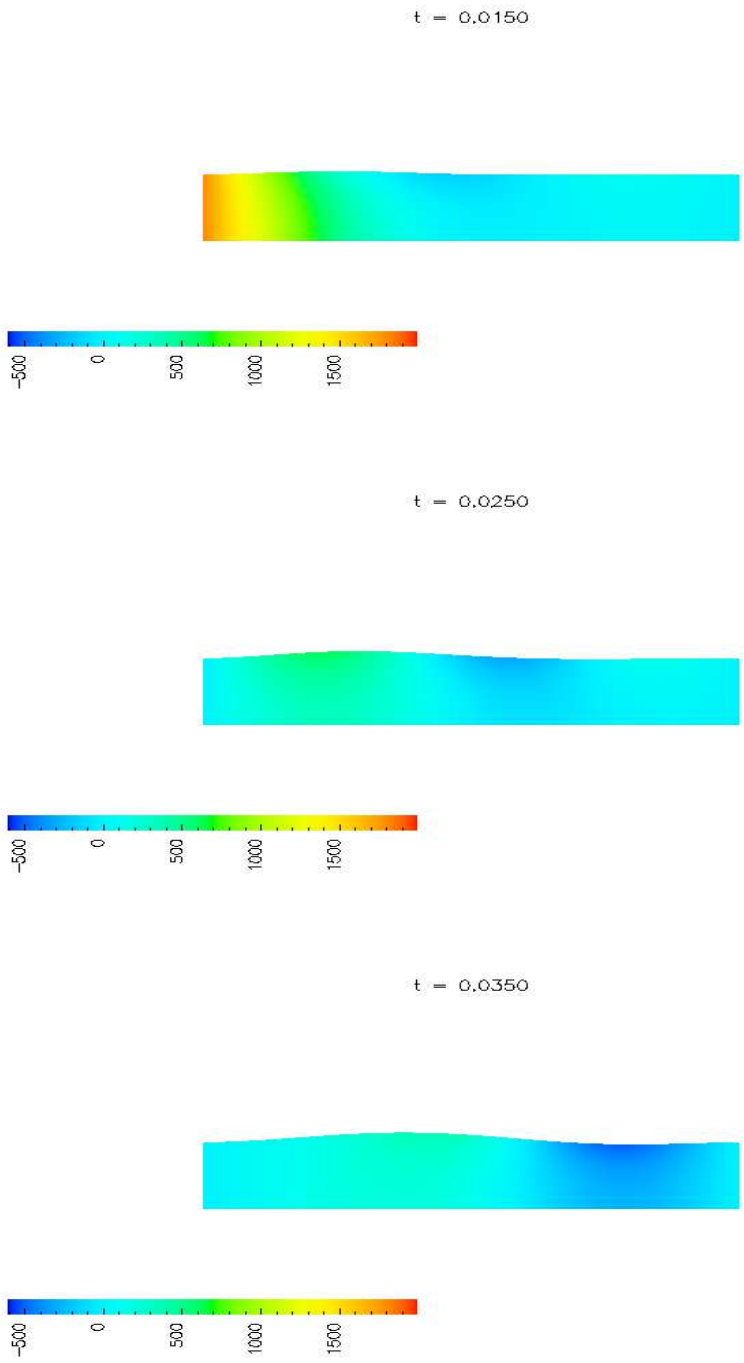


Fig. 5. Fluid pressure $[\frac{dynes}{cm^2}]$ at time instant $t = 0.015$ (top), $t = 0.025$ (middle), $t = 0.035$ (bottom)

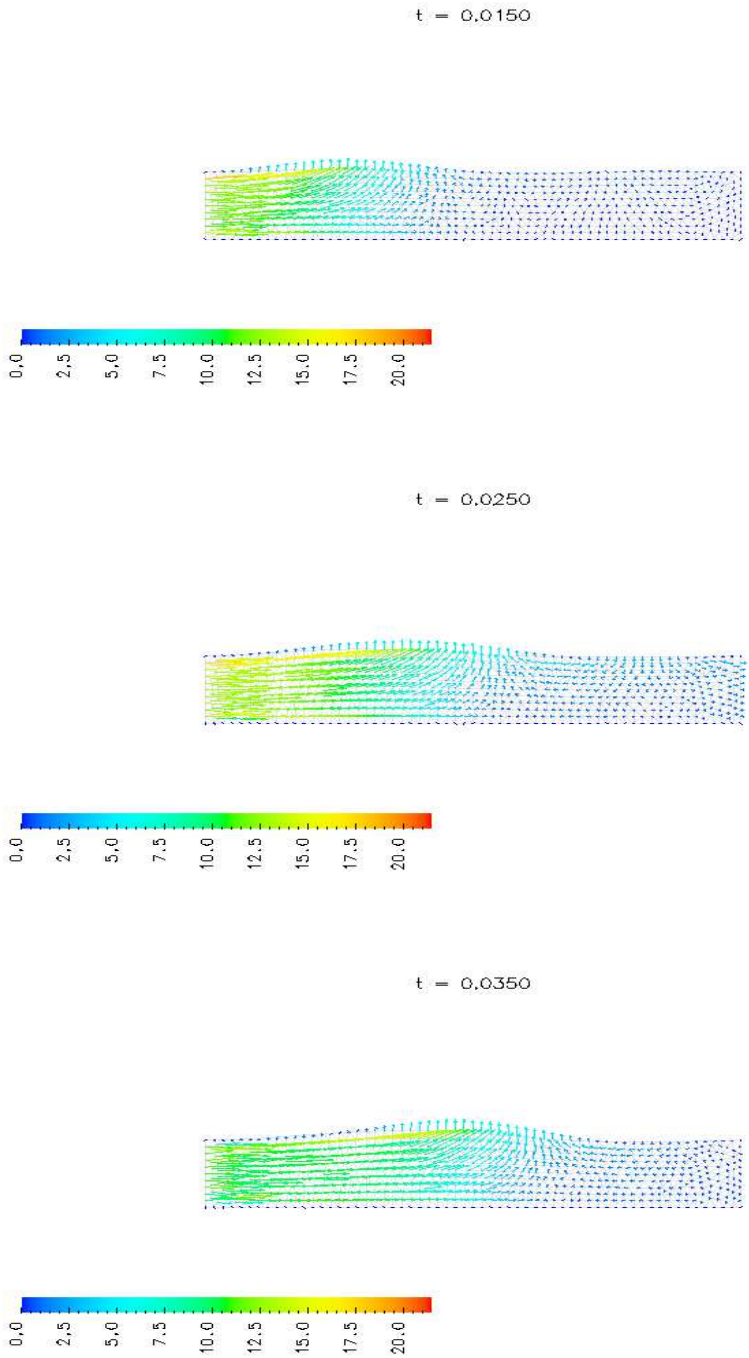


Fig. 6. Fluid velocity $[cm/s]$ at time instant $t = 0.015$ (top), $t = 0.025$ (middle), $t = 0.035$ (bottom)

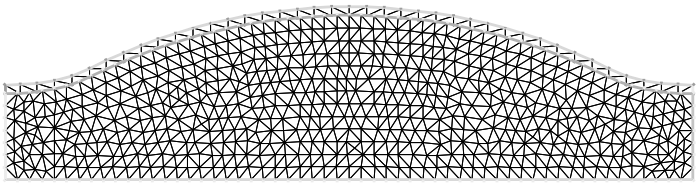

Fig. 7. Initial fluid and structure meshes

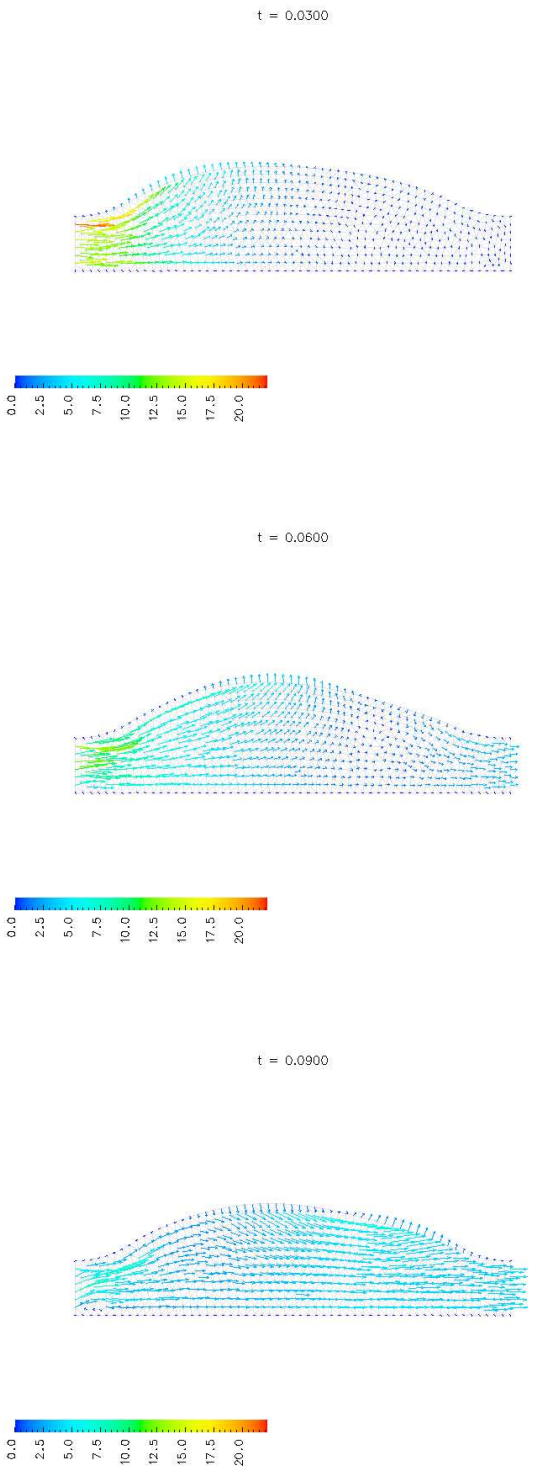


Fig. 8. Fluid velocity $[cm/s]$ at time instant $t = 0.030$ (top), $t = 0.060$ (middle), $t = 0.090$ (bottom)

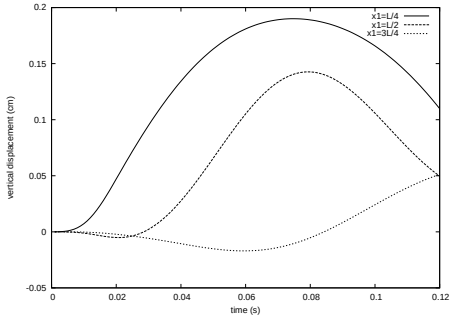


Fig. 9. Vertical displacement of three points at the interface of horizontal coordinates $x_1 = 1.5$, $x_1 = 3$, $x_1 = 4.5$. The left and right sides of the fluid domain have horizontal coordinates $x_1 = -1$ and $x_1 = 7$.